Published as Chapter 15 in the book
Molecular Interfacial Phenomena of Polymers and Biopolymers (Pu Chen, Editor)
Woodhead Publishing, Cambridge, UK, 2005; pp. 538-579.

Triblock Copolymers as Promoters of Solubilization of Oils in Aqueous Surfactant Solutions

Peter A. Kralchevsky and Nikolai D. Denkov

Laboratory of Chemical Physics & Engineering, Faculty of Chemistry, University of Sofia, Bulgaria

1. Introduction

The term 'solubilization' was introduced by McBain[1] to denote the increased solubility of a given compound, associated with the presence of surfactant micelles or inverted micelles in the solution. The most popular solubilization process is the transfer of oil molecules into the core of surfactant micelles. Thus, oil that has no solubility (or limited solubility) in the aqueous phase becomes water-soluble in the form of solubilizate inside the micelles. This process has a central importance for washing of oily deposits from solid surfaces and porous media, and for removal of oily contaminants dispersed in water. The great practical importance of solubilization is related to its application in the everyday life: in the personal care and household detergency, as well as in various industrial processes.[2]

The main actors in the solubilization process are the micelles of surfactant and/or copolymer. Their ability to uptake oil is of crucial importance.[2,3] The addition of copolymers, which form mixed micelles with the surfactants,[4] is a way to control and improve the micelle solubilization performance. Two main kinetic mechanisms of solubilization have been established, whose effectuation depends on the specific system:

Solubilization as a bulk reaction: Molecular dissolution and diffusion of oil into the aqueous phase takes place, with a subsequent uptake of oil molecules by surfactant micelles.[5–9] This mechanism is operative for oils (like benzene, hexane, etc.), which exhibit a sufficiently high solubility in pure water. Theoretical models have been developed and verified against the experiment.[6,8,9] Figure 1 illustrates the occurrence of the bulk solubilization. First, oil molecules are dissolved from the surface of an oil drop into water. Kinetically, this process can be characterized by a mass transfer coefficient. Next, by molecular diffusion, the oil molecules penetrate in the water phase, where they react with the micelles. Thus, the concentration of free oil molecules diminishes with the distance from the oil-water interface. In other words, the solubilization takes place in a restricted zone around the droplet, as shown schematically in Fig. 1.

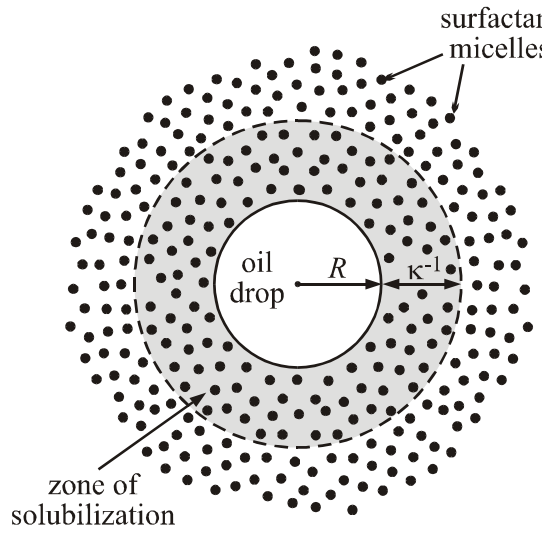

Figure 1. Solubilization as a bulk reaction: Sketch of an oil drop of radius *R* in a micellar surfactant solution. Oil molecules are dissolved from the surface of the drop into water. Molecular diffusion of oil into the water takes place, with a subsequent uptake of oil molecules by surfactant micelles. The solubilization occurs mostly in a narrow zone (shown shadowed) around the drop.[8]

Solubilization as a surface reaction. This is the major solubilization mechanism for oils that are practically insoluble in water.[5,7,10-18] The uptake of such oils cannot happen in the bulk of the aqueous phase. The solubilization can be realized only at the oil-water interface. The mechanism may include (i) micelle adsorption, (ii) uptake of oil, and (iii) desorption of the swollen micelles,[16-18] see Fig. 2. Correspondingly, the theoretical description of the process involves the rate constants of the three consecutive steps. If the empty micelles are long rodlike aggregates, upon solubilization they usually break to smaller spherical aggregates.[16,19] For some systems (mostly solid solubilizates), the intermediate stages in the solubilization process may involve penetration of surfactant solution into the oily phase and formation of a *liquid crystalline phase* at the interface.[20-24]

In the case of solubilization as surface reaction, the detailed kinetic mechanism could be multiform. Some authors[5,11] expect that the surfactant arrives at the interface in a monomeric form. Then, at the phase boundary mixed (or swollen) micellar aggregates are formed, which eventually desorb. This version of the model seems appropriate for solid solubilizates, because hemimicelles can be formed at their surfaces, even at surfactant concentrations below the bulk critical micellization concentration (cmc).[25] Another concept, presented by Plucinski and Nitsch,[13] includes a step of partial fusion of the micelles with the

oil-water interface, followed by a step of separation. Such mechanism could take place in the case when microemulsion drops, rather than micelles, are responsible for the occurrence of solubilization.

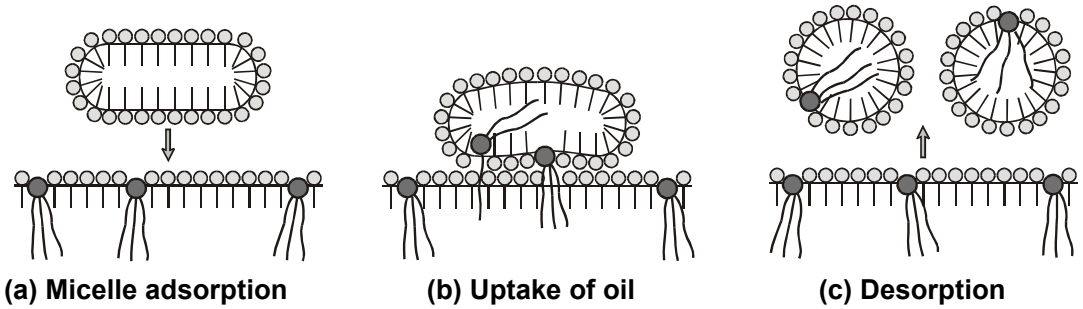

Figure 2. Solubilization as a surface reaction: The process can be modeled as a sequence of three steps: (a) adsorption of an empty micelle at the oil-water interface; (b) uptake of oil accomplished as a surface reaction: the empty micelle takes oil and splits into several swollen micelles; (c) desorption of the swollen micelles. The molecule with three tails (the solubilizate) represents schematically triglyceride.[17]

Experiments with various surfactant systems[14,18,26] showed that the solubilization rates for solutions of *ionic* surfactants are generally much lower than those for nonionic surfactants. This can be attributed to the electrostatic repulsion between the micelles and the similarly charged surfactant adsorption monolayer at the oil-water interface. On the other hand, copolymers have been found to form micelles, which solubilize well various hydrophobic compounds, even in the absence of low-molecular-weight surfactants.[27-35] Moreover, as shown in Refs. 16-18, appropriately chosen copolymers can act as very efficient promoters of the solubilization.

We have several aims in this chapter: First, to present models of the solubilization kinetics, which have been verified for surfactant/polymer systems. Second, to discuss the specific role of the copolymers as promoters of oil solubilization in the surfactant systems. Third, to demonstrate that the understanding of the detailed mechanism of solubilization may suggest productive ways for knowledge-based optimisation of the surfactant/polymer mixtures, with respect to the solubilization kinetics.

This chapter is organized as follows. In section 2 we present briefly the experimental methods to study solubilization. Section 3 is devoted to the kinetic mechanisms of solubilization. In section 4 we consider mixed micelles of nonionic surfactants and triblock copolymers, and the change in their size and shape upon solubilization. Next, in section 5 we

review data for the solubilization of triglycerides by mixed micelles of nonionic surfactants and copolymers. Finally, in section 6 we discuss the use of ionic surfactants, in mixture with copolymers and electrolytes, for solubilization of water-insoluble oils.

2. Experimental methods to study solubilization kinetics

2.1. Solubilization in emulsions

The kinetics of solubilization can be investigated in experiments with emulsions, which are subjected to agitation.[36-39] In this case, one way to detect the solubilization is to measure the emulsion turbidity. The solubilization rate can be characterized with the time necessary for the turbidity to level off.[36] More detailed kinetic information can be obtained if the time dependencies of the drop size and concentration are monitored by dynamic and static light scattering.[38,39] Another method to study solubilization kinetics with emulsions is to take samples from the shaken emulsion at selected times, and to subject these samples to phase separation using a centrifuge: the kinetics of solubilization can be characterized by the decrease of the volume of separated oily phase after the sample centrifugation.[37]

It should be noted that the interpretation of the experimental results on solubilization kinetics, obtained with batch emulsions, might face difficulties when there is flocculation, coalescence or Ostwald ripening in the system.

2.2. Solubilization with individual drops

The experiments on solubilization kinetics can be performed with single oil drops. This approach allows one to carry out precise measurements of the solubilization rate, as a function of various factors, such as oil type; drop size; temperature; type and concentration of surfactants, polymers, electrolytes, etc.

Carroll[5,40] developed a 'drop-on-fibre technique', which is based on measuring the time-dependence of the key dimensions of a drop, attached to a fibre, and having a constant non-zero contact angle. Ward[26] presented a comprehensive review of the results, obtained by this method.

An alternative technique, also dealing with single drops, was developed and applied by Miller and co-authors.[14,15,24] This is the so-called 'basic-oil-drop contacting procedure', in which a thin needle is used to inject small oil drops, typically 50-100 μm in diameter, into a

narrow rectangular glass capillary cell (of 400 μm inner width), which is pre-filled with the studied aqueous surfactant solution. The diminishing of each drop, as a result of the oil solubilization, is monitored by video-microscopy.

Similar experimental technique was used in our studies.[8,18] Briefly, the surfactant solution was loaded in a circular glass capillary of inner diameter 585 μm and length 50 mm (see Fig. 3).

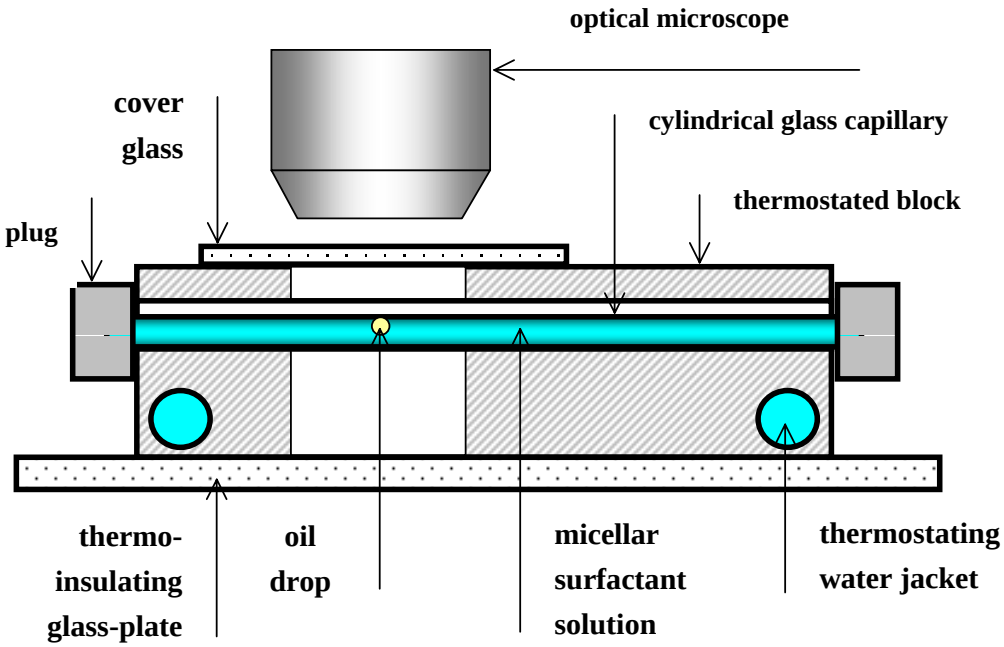

Figure 3. Setup for studying the kinetics of solubilization of single oil drops. The drops are placed in thermostated glass capillaries. The diminishing of drop radius with time, due to oil solubilization in the surfactant micelles, is monitored by optical microscopy.[18]

Next, an oil drop was injected in the capillary by means of a micro-syringe, with a custom-made, fine glass needle of outer diameter 45 μm. The initial drop radius was typically $R \leq 50$ μm. During the experiment, the capillary was held immobile in a horizontal channel, inside a thermostated metal block. The two ends of the capillary were plugged to prevent solution evaporation during the experiment. A metal block with 8 parallel channels was used, which allowed us to simultaneously perform experiments with 8 capillaries. Above each capillary, there was an opening, covered with a glass plate, which enabled us to observe microscopically the diminishing of each oil drop, due to solubilization. Optical microscope, equipped with long-focus objectives, was used.

The relatively small inner diameter of the capillary, and its horizontal position, are important for preventing the gravity-driven, free thermal convections in the surfactant solution.[41] If such convections are missing, the results are more reproducible and can be quantitatively interpreted by theoretical models, based on diffusion (or barrier-diffusion) transport of surfactant micelles and oil molecules. The latter advantage is very important, if one wants to reveal the actual mechanism of oil solubilization, by comparing the results from the kinetic experiments with the predictions of theoretical models.

To check whether thermal convections are present or absent, one can use a criterion based on the Rayleigh number:[42]

$$R_a \equiv g\beta_p \Theta h^3/(\nu\chi) \qquad [1]$$

Here h is the height of the liquid in the vessel, g is the acceleration due to gravity, $\beta_p = 2.27 \times 10^{-4}$ K^{-1} is the coefficient of thermal expansion of water, $\nu \approx 8.2 \times 10^{-3}$ cm^2/s is the kinematic viscosity of water, $\chi \approx 1.44 \times 10^{-3}$ cm^2/s is the thermal diffusivity of water, $\Theta \approx 0.1$ K is the characteristic temperature difference in the container in our experiments.[8,18] For $R_a \leq 1$ the free thermal convections are suppressed, whereas for $R_a > 1$ one could expect the appearance of such convections. For sub-millimetre in diameter capillaries, like those used by us, one estimates $R_a < 1$. Hence, the free thermal convections are suppressed, and the solubilization occurs under diffusion transport of the dissolved species. The latter allows us to interpret quantitatively the obtained data, see sections 3.1 and 5 below.

As an illustration of the fact that the thermal convections are negligible in the used capillary cell, in Fig. 4 we plot the experimental result for the diminishing of a benzene drop, injected in a surfactant solution at a concentration below the cmc (no micellar solubilization).[8]

Such a drop diminishes only due to the molecular dissolution of benzene into water. As shown theoretically in Ref 8, if convection is missing, the time dependence of the drop radius, $R(t)$, is described by the equation (see Eq [14] below):

$$R(t) = [1.8\,\beta_0\,(t_0 - t)]^{1/2} \qquad [2]$$

Here t_0 is the moment of drop disappearance, $R(t_0) = 0$; $\beta_0 = v_{oil}\,D_{oil}\,c_{eq} = 1.654 \times 10^{-8}$ cm^2/s is a known material parameter (v_{oil} is the volume of an oil molecule, D_{oil} is its diffusivity in water; c_{eq} is the equilibrium concentration of dissolved oil in water). As seen in Fig. 4, the experimental data agrees excellently with Eq. [2]; there are no adjustable parameters. This is a proof for the absence of free thermal convections in our capillary set-up (Fig. 3).[8]

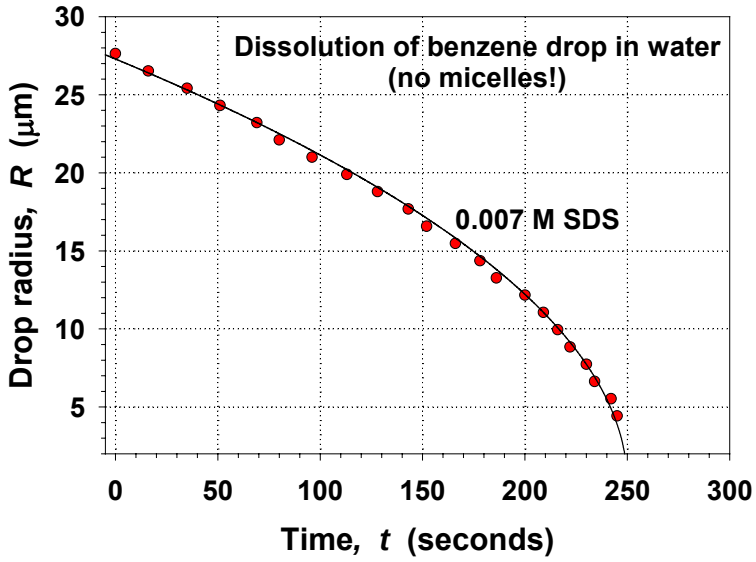

Figure 4. Plot of the radius, *R,* vs. time, *t*, for a benzene drop in water at 27°C (the method from Fig. 3 is used). The water contains 0.007 M sodium dodecyl sulfate (SDS), below the CMC, to stabilize the drop against attachment to the glass wall. The solid line is fit drawn by means of Eq [2]; no adjustable parameters.[8]

In some of our solubilization experiments, we used the experimental cell depicted in Fig. 5, which is much easier for manipulation. Surfactant solution (without oil drops) is placed in a thermostated glass container of dimensions $2 \times 2 \times 1.5$ cm (see Fig. 5).

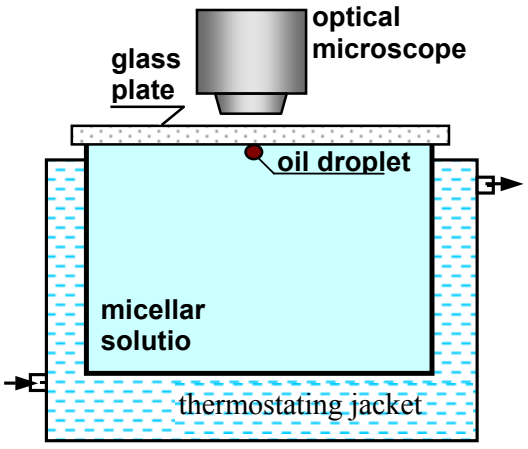

Figure 5. Set-up for investigating the rate of solubilization of single oil drop situated below glass/water interface by using optical microscopy. Due to the large size of the container with surfactant solution, it is impossible to avoid the appearance of free thermal convections in the system.[18]

In parallel, the oil drops are prepared in the form of diluted emulsion in the studied surfactant solution. By using a pipette, small portion of the emulsion is added to the micellar solution in the container, and the latter is covered by a glass plate. In this way, a number of oil drops are introduced in the cell. They emerge below the glass plate, due to the buoyancy force. The drop radius is typically around and below 30 μm. Due to solubilization, the drop size diminishes with time.

To illustrate the difference between the two used experimental cells, in Fig. 6 we present data for the solubilization rate of soybean-oil drops, as a function of the concentration of the triblock copolymer Synperonic L61, $E_{2.5}$-P_{34}-$E_{2.5}$, $M_w \approx 2100$; briefly, SL61. Here and hereafter 'E' stands for ethylene oxide group, and 'P' – for propylene oxide group. In Fig. 6 we characterize the solubilization rate by the slope of the curve dR/dt, which shows how rapidly the drop radius decreases with time. All drops have initial radius $R_0 \approx 35 \pm 5$ μm. As seen in Fig. 6, the data obtained with both cells indicate an increase of the solubilization rate with the concentration of the added SL61.

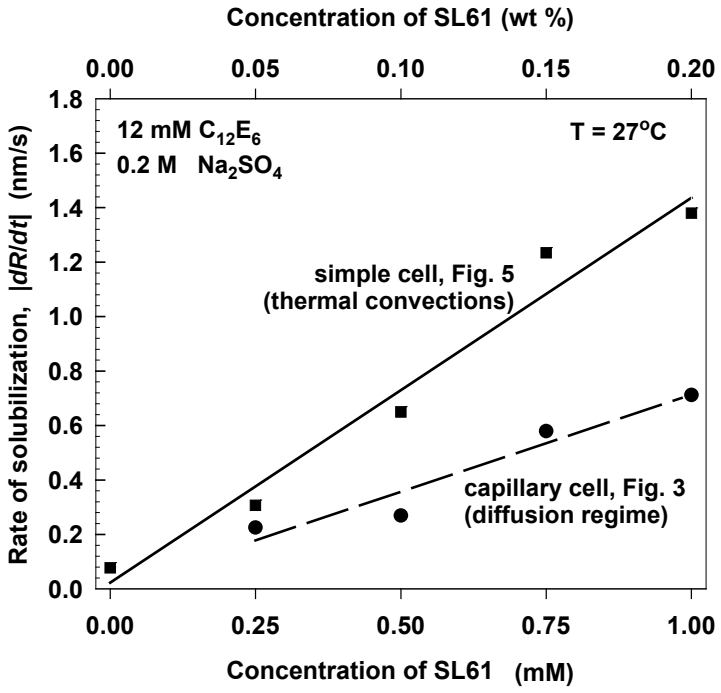

Figure 6. Comparison between the two experimental cells: Rate of solubilization of soybean oil as a function of the concentration of the triblock copolymer Synperonic L61. All solutions contain 12 mM $C_{12}E_6$ and 0.2 M Na_2SO_4. The temperature is 27 °C.[18]

However, the rates measured in the large cell are systematically greater than those obtained with the capillary cell. This difference can be attributed to the thermal convections in the large cell. The convections accelerate the transport of micelles, in comparison with the diffusion. However, such convections are engendered by small random temperature gradients, which are very difficult to control experimentally or to predict theoretically.

The estimates based on Eq [1] show that even with a fine control of the temperature, $\Theta \approx 0.1$ K, the Rayleigh number is $R_a \approx 10^4 >> 1$ for $h = 1.5$ cm, which means that it is virtually impossible to suppress the free convection by thermostating a centimetre-sized vessel. Because $R_a \propto h^3$, one could efficiently suppress the free convections by decreasing the height of the vessel, h, say, by using a capillary cell, like that in Fig. 3.

In conclusion, the capillary cell (Fig. 3) enables one to obtain experimental data on the kinetics of solubilization, which are liable to quantitative theoretical interpretation. The larger cell (Fig. 5) is much easier to operate and can be used for comparison of the relative rates of solubilization in various solutions. However, the results obtained with the latter cell are affected by uncontrollable thermal convection and they are not liable to quantitative interpretation.

3. Kinetic mechanisms of solubilization

3.1. The solubilization as a bulk reaction

As mentioned above, this kinetic regime of solubilization could be observed with oils that exhibit some solubility in pure water. Let us consider the process in Fig. 1. Each micelle is assumed to be capable to take up to M molecules of oil (in general, $M > 1$). If the solubilization occurs in a stationary regime, the concentration of dissolved oil, c_{oil}, obeys the equation[6,8]

$$D_{oil}\nabla^2 c_{oil} = k_+ c_a c_{oil} \qquad [3]$$

where D_{oil} is the diffusivity of oil molecules dissolved in water, c_a is the number concentration of active micelles, and k_+ is the rate constant of solubilization. Following Kabalnov and Weers[6], in Eq [3] we have approximately assumed that k_+ is the same for all active micelles (irrespective of whether or not they have already taken some oil molecules). (The active micelles are all micelles that are able to solubilize oil, i.e. all micelles except the entirely full

ones.) Further, for spherical symmetry (spherical drop of radius R, Fig. 1), Eq [3] can be represented in the form[6,8]

$$\frac{1}{r^2}\frac{d}{dr}\left(r^2\frac{dc_{\rm oil}}{dr}\right)=\kappa^2 c_{\rm oil}\ , \qquad [4]$$

$$\kappa^2 \equiv k_+ c_a / D_{\rm oil} \qquad [5]$$

In Eq [4], r is the radial coordinate; $r = R$ at the drop surface. If the micelle diffusion is sufficiently fast (in comparison with the process of solubilization), then one can expect that the active micelles leave the neighbourhood of the oil drop before becoming full micelles. In such case, the concentration of full micelles is (approximately) zero, and consequently, $c_a = c_{\rm tot}$ = const., where $c_{\rm tot}$ is the total micelle concentration. Then Eq [5] acquires the form

$$\kappa^2 = k_+ c_{\rm tot} / D_{\rm oil} = \text{const.} \qquad [6]$$

The boundary conditions for Eq. [4] are[8]

$$\frac{1}{\alpha_0}\frac{\partial c_{\rm oil}}{\partial r}\bigg|_{r=R} = c_{\rm oil}(R) - c_{\rm eq}\,, \qquad c_{\rm oil}\big|_{r\to\infty} = 0 \qquad [7]$$

where $c_{\rm eq}$ is the equilibrium solubility of the oil in water, and α_0 is a mass-transfer coefficient. The first Eq [7] states that the dissolution flux of oil into water is proportional to the difference between the subsurface local concentration of oil and the equilibrium (saturation) concentration of oil in water. For a large mass-transfer coefficient, $\alpha_0 >> 1$, the left-hand side of the first Eq [7] vanishes and it reduces to $c_{\rm oil}(R) = c_{\rm eq}$ = const. The solution of Eq [4], along with Eqs [6] and [7], reads

$$c_{\rm oil}(r) = \frac{c_{\rm eq} R}{1+(\kappa + R^{-1})/\alpha_0}\,\frac{\exp[\kappa(R-r)]}{r} \qquad [8]$$

Equation [8] shows that the quantity κ^{-1} determines the width of the "active zone" around the drop surface, where the solubilization takes place (see Fig. 1). With the help of Eq [8], one determines that the number of oil molecules dissolved in water per unit area of the drop surface, and per unit time, is:

$$Q_{\rm oil} = -D_{\rm oil}\frac{\partial c_{\rm oil}}{\partial r}\bigg|_{r=R} = \frac{\kappa + R^{-1}}{1+(\kappa + R^{-1})/\alpha_0} D_{\rm oil} c_{\rm eq} \qquad [9]$$

The decrease of the volume of the oil drop, V, with the time, t, is proportional to the flux of oil molecules across the whole drop surface, $4\pi R^2 Q_{\rm oil}$:

$$-\frac{dV}{dt} = \mathrm{v}_{\mathrm{oil}}(4\pi R^2)\lambda\, Q_{\mathrm{oil}} \qquad [10]$$

Here $\mathrm{v}_{\mathrm{oil}}$ is the volume per molecule in the oil phase and λ is a geometrical correction factor, which accounts for the fact that in our experiments the oil drop is located below the glass surface (the surface of the capillary, see Fig. 3), rather than in the bulk of the aqueous phase. The following expression for λ was derived in Ref 8:

$$\lambda = \frac{0.9 + 4.725\,\kappa R + 2.1(\kappa R)^2}{1 + 5.25\,\kappa R + 2.1(\kappa R)^2} \qquad [11]$$

Note that for $0 \le \kappa R < \infty$, we have $0.9 \le \lambda \le 1$, so in a first approximation one can work with $\lambda \approx 0.95$ = const. Substituting Eq [9] and $V = \frac{4}{3}\pi R^3$ in Eq [10], we obtain a differential equation for $R(t)$:[8]

$$\frac{dR}{dt} = -\frac{(1+\kappa R)\alpha_0\beta_0\lambda}{1+(\alpha_0+\kappa)R} \qquad [12]$$

where β_0 is a parameter, which is determined by the properties of the oil:

$$\beta_0 = \mathrm{v}_{\mathrm{oil}}\, D_{\mathrm{oil}}\, c_{\mathrm{eq}} \qquad [13]$$

By integration of Eq [12], one can obtain the theoretical dependence $R(t)$. Let us now consider some important special cases.

Molecular dissolution of oil (no solubilization). In this case, $k_+ = 0$, $\kappa = 0$, and then Eq [11] yields $\lambda = 0.9$. Furthermore, let us assume that the dissolution of oil at the drop surface is fast, i.e. $\alpha_0 R >> 1$. Then, Eq [12] reduces to:

$$\frac{dR}{dt} = -0.9\frac{\beta_0}{R} \qquad [14]$$

The integration of Eq [14] yields Eq [2], i.e. a square-root time-dependence, which has been found to agree excellently with experimental data for benzene drops, without using any adjustable parameters; see Fig. 4.

Narrow solubilization zone around the oil drop ($\kappa R >> 1$). In this limiting case, Eq [11] yields $\lambda = 1$ and Eq. [12] reduces to

$$-\frac{dR}{dt} \approx \frac{\alpha_0\beta_0\kappa}{\alpha_0+\kappa} \equiv u \qquad (\kappa R >> 1) \qquad [15]$$

where the constant parameter u has the meaning of solubilization rate. Integrating Eq [15] with a boundary condition $R(0) = R_0$, we get a linear time dependence:

$$R(t) \approx R_0 - u\,t \qquad (\kappa R >> 1) \qquad [16]$$

Such linear dependence was observed in experiments on solubilization of individual decane drops in sodium dodecyl sulfate (SDS) solutions, see Fig. 7.

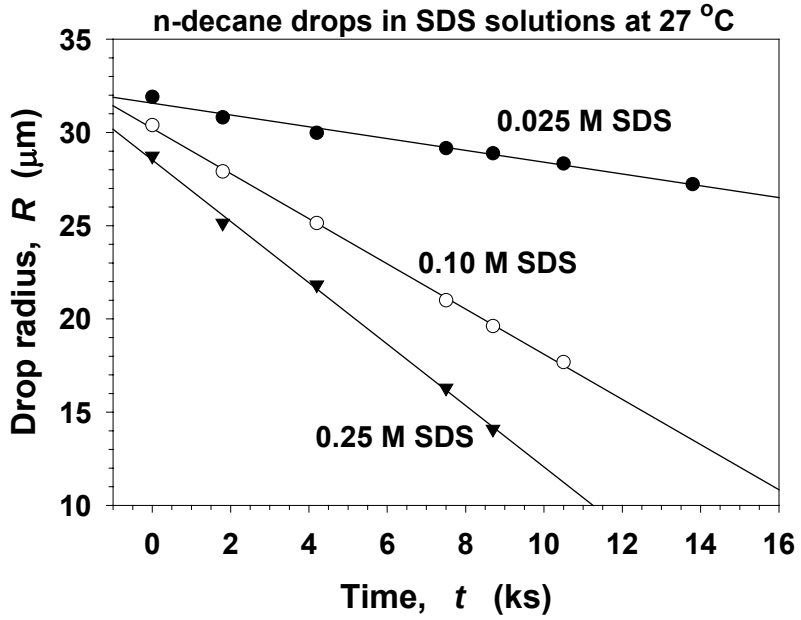

Figure 7. Plot of the radius, *R,* vs. time, *t*, for n-decane drops in micellar SDS solutions at 27 °C (SDS concentrations denoted in the figure). Each line corresponds to a separate diminishing drop; the linear regressions are drawn in accordance with Eq. [16].[8]

The slopes of the experimental lines give the solubilization rate, u, as a function of the surfactant concentration, c_s. In general, u increases with the rise of c_s. The latter dependence can be described with the help of Eqs [6] and [15]:[8]

$$u(c_s) = \frac{a(c_s - \mathrm{cmc})^{1/2}}{b + (c_s - \mathrm{cmc})^{1/2}}, \qquad [17]$$

where the constant parameters are:

$$a = \alpha_0\beta_0, \qquad b = (D_{oil}\, n_m\, \alpha_0^2 / k_+)^{1/2} \qquad [18]$$

n_m is the mean aggregation number of the micelles; the total number concentration of the micelles is $c_{tot} = (c_s - \mathrm{cmc})/n_m$. Equation [17] was found to describe well the experimental

dependence $u(c_s)$.[8] From the fit of the data, the following parameter values were determined for the system SDS/decane: mass-transfer coefficient $\alpha_0 = 30 \pm 6$ (μm^{-1}) and solubilization rate constant (uptake of oil by the micelles) $k_+ = (1.0 \pm 0.3) \times 10^{-13}$ (cm^3/s). Note that if the solubilization were purely diffusion limited, then k_+ would be much greater: $k_+ = 4\pi D_{oil} r_m \approx 2.4 \times 10^{-11}$ cm^3/s, where $r_m \approx 2.4$ nm is the radius of the SDS micelles.[43.] Hence, we may conclude that the elementary act of solubilization in the system SDS/decane happens under *barrier* control. One possible explanation of this barrier is that the oil molecules in water are 'wrapped' by a shell of structured water molecules. (Such shell is believed to be responsible for the hydrophobic surface force.[44,45]) Thus, the barrier could be related to the destruction of this shell before the engulfment of an oil molecule by the micelle. See Ref 8 for details.

Fast dissolution of oil ($\alpha_0 \to \infty$). As already mentioned, in such a limiting case the subsurface concentration of oil becomes equal to the respective equilibrium (saturation) concentration, $c_{oil}(R) = c_{eq} = \text{const}$. In the same limit, $\alpha_0 \to \infty$, Eq. [12] reduces to

$$\frac{dR}{dt} = -\frac{\beta_0 \lambda}{R}(1 + \kappa R) \qquad [19]$$

The integration of Eq [19] for $\lambda \approx$ const., along with the boundary condition $R(0) = R_0$, yields:

$$R(t) = R_0 + \frac{1}{\kappa} \ln\left(\frac{\kappa R + 1}{\kappa R_0 + 1}\right) - \kappa \lambda \beta_0 \, t \qquad [20]$$

For fits of experimental data, it is convenient to use the inverted dependence:

$$t(R) = [R_0 + \frac{1}{\kappa} \ln\left(\frac{\kappa R + 1}{\kappa R_0 + 1}\right) - R]/(\kappa \lambda \beta_0) \qquad [21]$$

For the solubilization of benzene in SDS micellar solutions, the best fits are shown in Fig. 8. They are obtained by means of the least squares method, treating κ and R_0 as two adjustable parameters. A very good agreement between the theoretical model and the experimental data was obtained.

Note that Eqs [19]–[21] are derived using the assumption that the concentration of the full micelles is negligible. However, in the case of fast oil dissolution ($\alpha_0 \to \infty$), it may happen that a considerable fraction of the micelles become full. This will lead to a deceleration of the solubilization in comparison with the predictions of the above model. In such case, to interpret the experimental data, one could apply the detailed theory developed by Sailaja et al.,[9] which is based on population balance equations for the micelles.

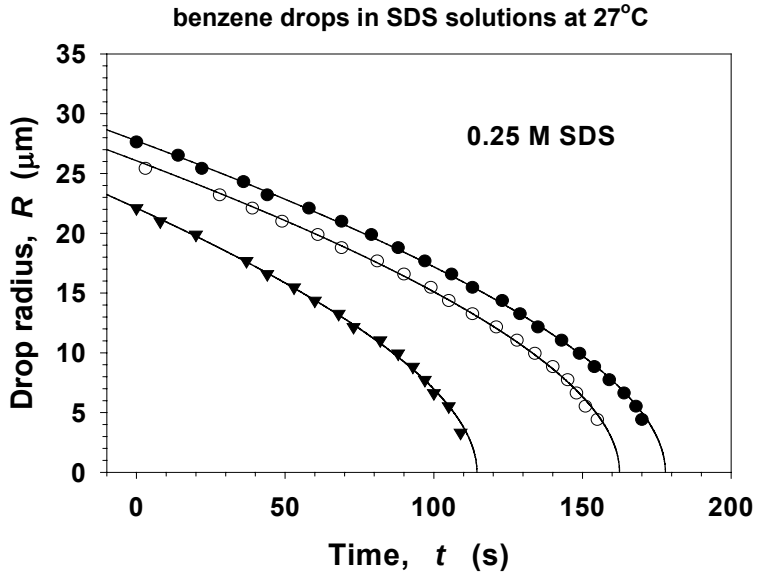

Figure 8. Plot of the radius, *R,* vs. time, *t*, for benzene drops in 0.25 M micellar solution of SDS at 27°C; set-up from Fig. 3. Each curve corresponds to a separate diminishing drop; the theoretical fits are drawn with the help of Eq [21].[8]

3.2. The solubilization as a surface reaction

Basic assumptions and equations. This is the only solubilization mechanism for oils (like the triglycerides), which have negligible solubility in pure water. The experiments[17,18] indicate that the elementary act of solubilization includes the following three consecutive steps (Figure 2):

(a) *Adsorption* of an empty micelle at the oil-water interface;

(b) *Uptake of oil*, accomplished by the surface reaction:

$$\{\text{empty micelle}\} + \{\text{oil molecules}\} = m\{\text{swollen micelles}\} \qquad [22]$$

(c) *Desorption* of the swollen micelles.

Equation [22] takes into account the experimental fact that the long cylindrical empty micelles split into m smaller aggregates (cylindrical or spherical) in the course of solubilization. Note that the micelles (empty and swollen) are not monodisperse in size, so that m is an average value. In particular, m varies from 1.8 to 5.4 for the mixed surfactant-polymer micelles investigated in Ref 16.

In the framework of the Langmuir adsorption model, we have:

$$\theta_0 + m\frac{\Gamma_1}{\Gamma_\infty} + \frac{\Gamma_2}{\Gamma_\infty} = 1 \qquad [23]$$

Here and hereafter, the index 1 denotes empty micelles, and index 2 – swollen micelles; Γ_1 and Γ_2 are the respective adsorptions of micelles at the oil-water interface (number of micelles per unit area); θ_0 is the area fraction of the empty adsorption sites; Γ_2/Γ_∞ and $m\Gamma_1/\Gamma_\infty$ are, respectively, the area fractions occupied by swollen and empty micelles. In Eq [23], we have taken into account that an empty micelle occupies an area that is m-times greater than the respective area per swollen micelle; Γ_∞^{-1} is the area per adsorption site. The net adsorption fluxes of empty and swollen micelles (number of micelles adsorbing per unit area and per unit time) are[46]

$$Q_1 = k_{1,\mathrm{a}}\, c_{1\mathrm{s}}\, \theta_0^m - k_{1,\mathrm{d}}\, \Gamma_1 \qquad [24]$$

$$Q_2 = k_{2,\mathrm{a}}\, c_{2\mathrm{s}}\, \theta_0 - k_{2,\mathrm{d}}\, \Gamma_2 \qquad [25]$$

Here $k_{i,\mathrm{a}}$ and $k_{i,\mathrm{d}}$ are the kinetic constants of adsorption and desorption of empty ($i = 1$) and swollen ($i = 2$) micelles; $c_{i\mathrm{s}} \equiv c_i(r{=}R)$, $i = 1,2$, are the "subsurface" concentrations of the empty and swollen micelles. The function $c_i(r)$, $r \geq R$, denotes the radial dependence of the concentration of the respective diffusing micelles around a spherical oil drop of radius R; the coordinate origin, $r = 0$, is fixed at the drop centre. In general, $c_{1\mathrm{s}}$ and $c_{2\mathrm{s}}$ differ from the respective bulk micelle concentrations, c_{10} and c_{20}, due to the diffusion and the surface reaction (solubilization), see Eq [29]. The surface mass balances of empty and swollen micelles can be expressed in the form

$$\frac{d\Gamma_1}{dt} = -k_{\mathrm{s}}\Gamma_1 + Q_1\,, \qquad \frac{d\Gamma_2}{dt} = mk_{\mathrm{s}}\Gamma_1 + Q_2 \qquad [26]$$

where k_{s} is the rate constant of solubilization, i.e. of the surface reaction described by Eq [22]. Equation [26] presumes that the solubilization is an *irreversible* process. In a *stationary* regime, ($d\Gamma_i / dt = 0$) Eq [26] yields:

$$Q_1 = k_{\mathrm{s}}\Gamma_1\,, \quad Q_2 = -mk_{\mathrm{s}}\Gamma_1\,, \quad \text{hence} \quad Q_2 = -m\,Q_1 \qquad [27]$$

Next, let us consider a spherical oil drop of radius R. In a stationary regime, the concentration distribution of the empty and swollen micelles around the drop is described by the equation

$$c_i(r) = c_{i0} - \frac{Q_i R^2}{D_i r} \qquad (i = 1, 2) \qquad [28]$$

where D_i is the micelle diffusion coefficient. Equation [28] is the solution of the stationary diffusion equation $\frac{d}{dr}\left(r^2\frac{dc_i}{dr}\right)=0$, satisfying the boundary conditions $c_i(r\to\infty) = c_{i0}$ and $D_i(\partial c_i/\partial r)_{r=R} = Q_i$. From Eq [28] it follows that the subsurface concentrations of the empty and swollen micelles are

$$c_{is} = c_i\big|_{r=R} = c_{i0} - \frac{R}{D_i}Q_i \qquad (i = 1, 2) \qquad [29]$$

Equations [23]–[26] and [29] form a system of 7 equations for determining the 7 unknown variables: Q_1, Q_2, Γ_1, Γ_2, c_{1s}, c_{2s} and θ_0. In particular, this system of equations determines the dependence $Q_1 = Q_1(R)$.

The decrease of the oil-drop volume, V, with time, t, during solubilization is due to the flux of full micelles, each of them carrying away a certain volume of oil, v_1. Thus, the balance of oil becomes:

$$-\frac{dV}{dt} = v_1\lambda(4\pi R^2)(-Q_2) \qquad [30]$$

As before, λ is a geometrical correction factor, which accounts for the fact that in our experiments the oil drop is situated in the vicinity of a glass surface (see Fig. 3), rather than in the bulk of the aqueous phase. In Ref 17, we have shown that one can set $\lambda = 0.9$. Substituting $Q_2 = -m\,Q_1$ and $V = \frac{4}{3}\pi R^3$ in Eq [30], we obtain a differential equation for $R(t)$:

$$\frac{dR}{dt} = -\lambda m\, v_1\, Q_1(R) \qquad [31]$$

In principle, Eq [31], with $Q_1(R)$ determined from Eqs [23]–[26] and [29], enables one to interpret theoretically the experimental dependence $R(t)$. Below we consider the simpler (but physically important) case of solubilization in Henry regime (low micelle adsorption), in which the set of equations can be linearized and the expression for $R(t)$ can be obtained in a convenient explicit form.

Solubilization of triglycerides in Henry regime. The experiment shows that for the systems investigated in Refs 16–18 ($C_{12}E_n$ + SL61), the rate of solubilization grows almost linearly with the increase of the micelle concentration. In the studied concentration range, the experimental curves do not exhibit a tendency for saturation (levelling off) at the higher surfactant concentrations. This indicates the occurrence of micelle adsorption in Henry

regime. In other words, the occupancy of the oil-water interface with adsorbed micelles is relatively low. Hence, in view of Eq [23], we obtain

$$m\frac{\Gamma_1}{\Gamma_\infty}+\frac{\Gamma_2}{\Gamma_\infty}<<1, \qquad \text{i.e.} \qquad \theta_0\approx 1 \qquad [32]$$

Setting $\theta_0 \approx 1$ in Eqs [24]–[25] and using Eq [27], we obtain a set of two linear equations for Γ_1 and Γ_2, whose solution reads:

$$\Gamma_1=\frac{k_{1,\mathrm{a}}}{k_\mathrm{s}+k_{1,\mathrm{d}}}\,c_{1s}, \qquad \Gamma_2=\frac{k_{2,\mathrm{a}}}{k_{2,\mathrm{d}}}\,c_{2s}+\frac{m k_\mathrm{s} k_{1,\mathrm{a}}}{k_\mathrm{s}+k_{1,\mathrm{d}}}\,c_{1s}, \qquad [33]$$

Next, combining Eqs [27] and [33], we obtain an expression for the stationary adsorption flux of empty micelles:

$$Q_1=k_\mathrm{s}\Gamma_1=\chi c_{1s}, \qquad \chi\equiv\frac{k_\mathrm{s}\,k_{1,\mathrm{a}}}{k_\mathrm{s}+k_{1,\mathrm{d}}} \qquad [34]$$

χ has the meaning of a compound rate-constant of solubilization. Furthermore, eliminating $c_{1\mathrm{s}}$ between Eqs [29] and [34] we get the explicit dependence $Q_1(R)$:

$$Q_1=\frac{\chi c_{10}}{1+\chi R/D_1} \qquad [35]$$

Finally, we substitute Eq [35] into Eq [31], and bring the result in the form[17]

$$\frac{dR}{dt}=-\frac{\alpha}{1+(\beta/\alpha)R} \qquad [36]$$

where

$$\alpha=\lambda m\,\mathrm{v}_1\chi c_{10}, \qquad [37]$$

$$\beta=\lambda m\,\mathrm{v}_1\chi^2 c_{10}/D_1=\frac{\alpha^2}{\lambda m\mathrm{v}_1 c_{10}D_1} \qquad [38]$$

The integration of Eq [36] yields:

$$R(t)=\frac{\alpha}{\beta}\{[1+2\beta(t_0-t)]^{1/2}-1\} \qquad (t\le t_0) \qquad [39]$$

In Eq [39] we have determined the integration constant from the boundary condition $R(t_0) = 0$, where t_0 is the moment of disappearance of the diminishing oil drop in the actual experiment. The square-root time-dependence, $R(t)$, in Eq [39] resembles the law of

diminishing of a liquid drop upon molecular dissolution into another liquid (say benzene in water), Eq [2], although the functional form and the parameter meaning are somewhat different.

By fitting the experimental data for $R(t)$ with the help of Eq [39] one can determine the parameters α and β. Next, from the values of α and β one can calculate the average number of oil molecules solubilized in a swollen micelle, n_s, and the kinetic parameter χ:

$$n_s \equiv \frac{v_1}{v_o} = \frac{1}{\lambda m c_{10} D_1 v_o} \frac{\alpha^2}{\beta}, \qquad \chi = \frac{\beta}{\alpha} D_1 \qquad [40]$$

where v_o denotes the volume of an oil molecule. Note that $c_{10} = (c_s - \text{cmc})/N_{\text{surfact}}$, where c_s is the total surfactant concentration and N_{surfact} is the number of surfactant molecules per empty micelle, see the next section. As shown in Fig. 9, Eq 39 provides excellent fits of solubilization data for triolein drops in mixed solutions of the triblock copolymer SL61 and the nonionic surfactant $C_{12}E_6$. Here and hereafter, C_{12} denotes dodecyl group and, as usual, 'E' denotes ethylene oxide group. The values of χ, determined from the fits, indicate that the copolymer SL61 acts as a promoter of solubilization, see Section 5.

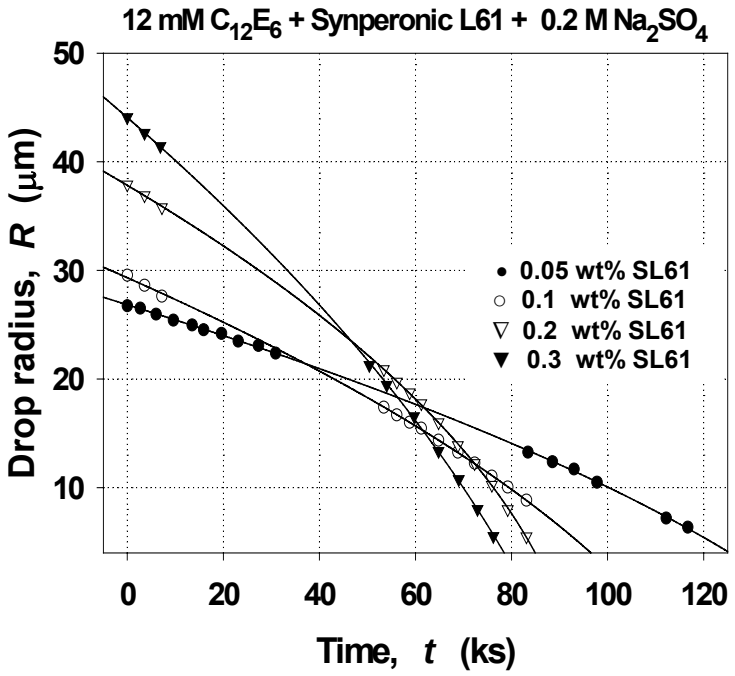

Figure 9. Plots of the radius, R, of triolein drops vs. time, t (1 ks = 1000 s): results from solubilization experiments in the capillary cell (Fig. 3) at temperature 27°C and various concentrations of SL61 denoted in the figure. The micellar solutions contain 12 mM $C_{12}E_6$ + 0.2 M Na_2SO_4 + SL61; the lines are best fits by means of Eq [39].[18]

4. Micelle transformations upon solubilization

4.1. Physicochemical background

In a series of experiments[16,18] on triglyceride solubilization, we studied the solubilization of triolein (as a representative of the triglycerides) by nonionic surfactants $C_{12}E_n$ (n = 5 or 6) and nonionic triblock copolymer SL61 ($E_{2.5}P_{34}E_{2.5}$). (Similar solubilization performance has Synperonic L81, E_3-P_{44}-E_3, $M_w \approx 2750$.) The nonionic surfactants, $C_{12}E_n$ (n = 5 or 6), were chosen because they solubilize triglycerides, at a detectable rate, even at room temperature. To reduce the cloud point of $C_{12}E_6$ and to accelerate the solubilization process, we added 0.2 M Na_2SO_4 to the solutions of this surfactant.

We applied light scattering and NMR techniques to determine how the micelle properties (such as aggregation number, size, shape, diffusion coefficient, number concentration, as well as the number of solubilized oil molecules per one micelle) varied in the course of solubilization.[16] The obtained data were used[17,18] for development and testing the respective theoretical model (Section 3.2). In addition, the micellar transformations during solubilization are a subject of independent interest.[47-60]

It was established by several research groups that different oils affect in different ways the surfactant micelles. The aliphatic hydrocarbons were found[48,52,53,56] to increase the micelle radius when the initial, empty micelles had spherical shape. However, when the initial empty micelles were relatively large and non-spherical (e.g., rods or worm-like aggregates) the solubilization of alkanes often led to a rod-to-sphere transition, accompanied with a significant decrease of the micellar size and aggregation number.[49,55] All these observations were explained by the predominant incorporation of alkanes inside the hydrophobic core of the micelles.

In contrast, amphiphilic substances, such as alkanols and amines, are solubilized with their polar groups being preferentially located at the water-hydrocarbon boundary of the micelle, in the so-called 'palisade layer'.[47,49-51,56,61,62] These substances reduce the surface charge density of the micelles, and thereby promote the formation of aggregates with shape corresponding to lower mean curvature (rods, disks). Similar effects were observed when aromatic hydrocarbons were solubilized by cationic micelles.[54,57-60] This was explained by a specific interaction between the positively charged head-groups of the surfactant and the highly polarizable π-electrons of the aromatic ring. This specific interaction leads to a

preferential location of the aromatic hydrocarbons at the surface of the cationic micelles, at least for not-too-high loading of the micelles with solubilizate.

The triglyceride molecules have three long hydrocarbon tails connected to a polar group. This molecular structure does not allow one to predict in advance what would be the effect of triglycerides on the micelle size and shape. The voluminous hydrocarbon tails render the triglyceride properties similar to those of the aliphatic substances, whereas the glyceride polar group could induce some specific interaction with the surfactant head-groups.

4.2. Experimental methods for investigating empty and swollen micelles

Dynamic light scattering (DLS) was used[16] for measuring the translational diffusion coefficient of the micelles and for determination of their hydrodynamic (Stokes) diameter, d_h. The latter was calculated[63] from the measured diffusion coefficient, D, by the Stokes-Einstein formula

$$d_h = kT / (3\pi\eta D) \qquad [41]$$

where η is the viscosity of the disperse medium (water), T is the absolute temperature, and k is the Boltzmann constant.

Static light scattering (SLS) was used for determination of the molecular mass, M_p, and the aggregation number, ν, of the micelles. For reasons explained in Ref 16, we determined the mass of the micelles, and the respective aggregation number, from the relation:[64]

$$M_p = \frac{R_h(\theta \to 0)}{cK} \qquad [42]$$

where $c = c_s$ − cmc (c_s is the total surfactant concentration, cmc is the critical micelle concentration); θ is the scattering angle, and $R_h(\theta)$ is the so-called Rayleigh ratio, which is proportional to the intensity of the scattered light; K is an optical constant:

$$K = \frac{4\pi^2}{N_A}\frac{n_0^2}{\lambda_w^4}\left(\frac{dn}{dc}\right)^2 \qquad [43]$$

N_A is the Avogadro number; λ_w is the wavelength of the illuminating light, n_0 and n are the refractive indices of the solvent (water) and the solution; dn/dc is the refractive index increment (measured independently by refractometer).

Our light scattering measurements[16] were performed at 27 °C by means of system 4700C Malvern Instruments (UK), equipped with an argon laser, operating at λ_w = 488 nm with a vertically polarized incident beam. In addition, we used nuclear magnetic resonance (NMR) techniques to determine the amount of solubilized triolein in the micelles. For this purpose, the molar ratio triolein/$C_{12}E_n$ was determined from the areas of selected, well-resolved peaks in the ^{1}H NMR spectra of the swollen micelles (see Ref 16 for details). The spectra were recorded on a Bruker DRX-250 NMR spectrometer, operating at 250 MHz for protons, using a dual ^{1}H/^{13}C probehead.

To interpret the data, we made the following two assumptions: (1) the micelles have the shape of prolate ellipsoids; (2) the ratio of $C_{12}E_n$/SL61 in the micelles is equal to their ratio in the dissolved surfactant mixture. The latter assumption implies that a single type of mixed micelles is formed in the $C_{12}E_n$/SL61 mixture, i.e. that there is no segregation of the micelles into $C_{12}E_n$ and SL61 enriched ones. Note that these assumptions are only used to characterize the change of the micelle shape, as a result of oil solubilization. Most of the micelle characteristics (aggregation number, total number concentration, diffusion coefficient, and number of oil molecules per one micelle), are directly determined by the applied experimental methods, and are not influenced by the above two assumptions.

To determine the micelle shape and composition, the following procedure was used. The total mass, M_p, of the surfactant molecules ($C_{12}E_5$ or $C_{12}E_6$), incorporated in one micelle, was determined by SLS; see Eq [42]. The relative molar ratio of $C_{12}E_n$ and SL61 in the micelles is calculated by using the assumption 2. Then the volume of the *hydrophobic part* of the surfactant molecules included in a micelle, V_{HPB}, was calculated from the mass of the aliphatic chains of the $C_{12}E_n$ molecules, plus the polyoxypropylene chains of the SL61 molecules, incorporated in one micelle (Figure 10).

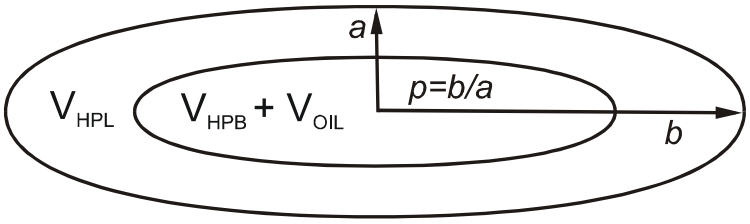

Figure 10. Schematic presentation of a swollen micelle, which has the shape of prolate ellipsoid with semi-axes *a* and *b*. V_{HPB} + V_{OIL} is the volume of the hydrophobic core of the micelle (hydrophobic portions of the surfactant and polymer molecules), while V_{HPL} is the volume of the hydrophilic headgroup region.

The mass density of the hydrophobic part was taken 0.9 g/cm^3 in these calculations. From the NMR measurements, we know the molar ratio $C_{12}E_n$/triolein in the micelle, which allowed us to calculate the number of triolein molecules per micelle and the respective volume, V_{OIL}, occupied by the triolein in a swollen micelle.

To obtain the volume of the *hydrophilic coat* of the micelle we calculated the mass of EO-groups per micelle. On the basis of literature results,[65,66] we assume that each ethoxy group binds 2 water molecules. Thus we can determine the total mass of the hydrophilic coat and assuming a mass density of ≈ 1 g/cm^3, to calculate the respective volume, V_{HPL}. The total volume of the micelle is $V_{MIC} = V_{HPL} + V_{HPB} + V_{OIL}$ (Figure 10).

The assumption that the micelles have the shape of a prolate ellipsoid allows us to determine the semiaxes, a and b, from the volume of the micelles, V_{MIC}, and from their diffusion coefficient, D, determined by DLS. Note that the hydrodynamic diameter, d_h, calculated by eq 41, is an effective particle diameter, which has a value between $2a$ and $2b$. The ratio of the large to the small axis, $p = b/a$, is determined from the experimental data for V_{MIC} and d_h, as an adjustable parameter. This aspect ratio, p, is related to the diffusion coefficient of the ellipsoid through the expression[55,67]

$$D = \frac{kT}{24\pi\eta a}\left(3ps + \frac{p}{2}\alpha_{II} + \frac{\alpha_I}{p}\right) \qquad [45]$$

$$s = \frac{\operatorname{arcosh}(p)}{p\left(p^2-1\right)^{1/2}} \qquad \text{for } p > 1 \text{ (prolate ellipsoid)} \qquad [46]$$

α_{II} and α_I are the mobility functions for the ellipsoid in directions parallel and perpendicular to the main axis, respectively: [67]

$$\alpha_{II} = \frac{2\left(p^2 s - 1\right)}{p^2 - 1} \quad , \quad \alpha_I = \frac{p^2\left(1 - s\right)}{p^2 - 1} \qquad [47]$$

The small semi-axis, a, can be expressed through the micellar volume:

$$a = \left(\frac{3V_{MIC}}{4\pi p}\right)^{1/3} \qquad [48]$$

Equations [45]-[48] allow one to determine p from the comparison of the experimentally measured diffusion coefficient with the theoretically calculated one, if the micelle volume is known. Thus one can restore the shape of the micelle from light scattering and NMR data.

4.3. Data for the empty and swollen micelles of $C_{12}E_n$ + SL61

Micelle size. Experimental data from Refs 16 and 18 are shown in Tables 1 and 2, and in Figs. 11–14. The values of D_1 in Table 1 are directly obtained by dynamic light scattering. To determine the bulk number concentration of empty micelles in the solution, c_{10} (a parameter that enters Eq 40), we first determined the number of surfactant molecules per micelle, $N_{surfact}$, by static light scattering (Table 2). Then we calculated $c_{10} = (c_s - \text{cmc})/N_{surfact}$, where c_s is the total surfactant concentration.

To illustrate the values in Table 1, in Fig. 11 we present the effective hydrodynamic diameter, d_h, which is defined by means of the Stokes-Einstein formula, Eq. [41]. In fact, d_h is the diameter of an imaginary spherical particle, which has the same diffusivity D_1 as the real elongated micelle. Figure 11 shows that the micelle size considerably decreases with the rise of the SL61 concentration.

Table 1. Experimental parameters for the empty micelles.

Synperonic L61 C_{SL61} [wt %]	diffusivity D_1 [cm^2/s]	micelle diameter d_h [nm], Eq [41]	micelle concen-tration c_{10} [cm^{-3}]
(a) Solutions of 0.012 M $C_{12}E_5$ + 0.01 M NaCl			
0.0	0.912×10^{-7}	47.7	–
0.1	1.49×10^{-7}	34.7	3.91×10^{15}
0.2	1.93×10^{-7}	26.8	8.04×10^{15}
0.3	2.15×10^{-7}	24	9.95×10^{15}
(b) Solutions of 0.012 M $C_{12}E_6$ + 0.2 M Na_2SO_4			
0	2.20×10^{-7}	23.5	0.71×10^{16}
0.04	2.61×10^{-7}	19.8	0.98×10^{16}
0.05	2.71×10^{-7}	19.1	1.05×10^{16}
0.08	2.99×10^{-7}	17.3	1.27×10^{16}
0.10	3.08×10^{-7}	16.8	1.39×10^{16}
0.15	3.3×10^{-7}	15.5	1.70×10^{16}
0.20	3.45×10^{-7}	14.7	2.02×10^{16}

Moreover, the empty micelles in the investigated solutions of $C_{12}E_5$ are markedly larger than those in the solutions of $C_{12}E_6$. Note, that as a rule, $C_{12}E_5$ forms bigger micelles than $C_{12}E_6$, despite of the lower ionic strength in the $C_{12}E_5$ solutions. This is due to the smaller hydrophilic head of the $C_{12}E_5$ molecules, which tend to form aggregates of smaller curvature

and bigger size (as compared to $C_{12}E_6$). DLS experiments show that the micelle size diminishes also during the solubilization (uptake of triolein). After 7-8 days of solubilization, the micelles reach their final size ($d_h \approx$ 8-10 nm, spherical or slightly elongated micelles), which is almost the same for all investigated systems, independently of the used concentrations of surfactant and SL61. Only for the solutions of $C_{12}E_6$ without SL61, we had to make measurements after the 16th day of contact with triolein, because the solubilization in this system is very slow: the accelerating effect of SL61 is missing.

(a)

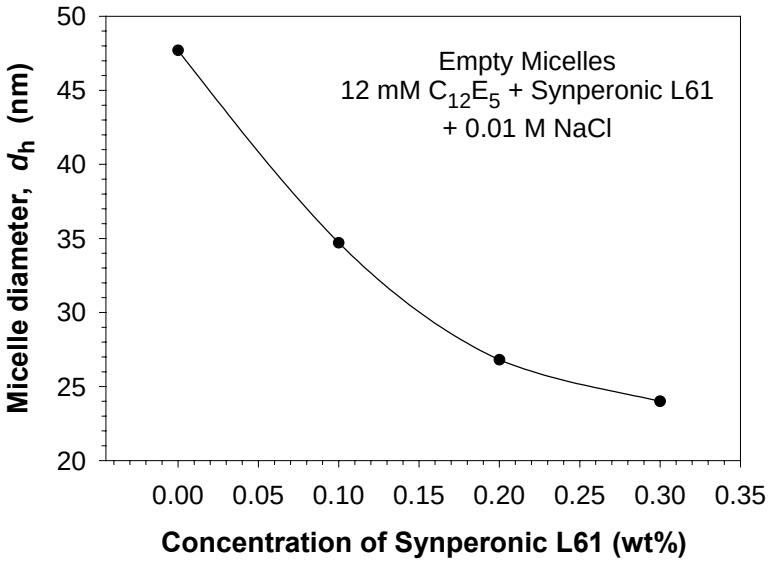

(b)

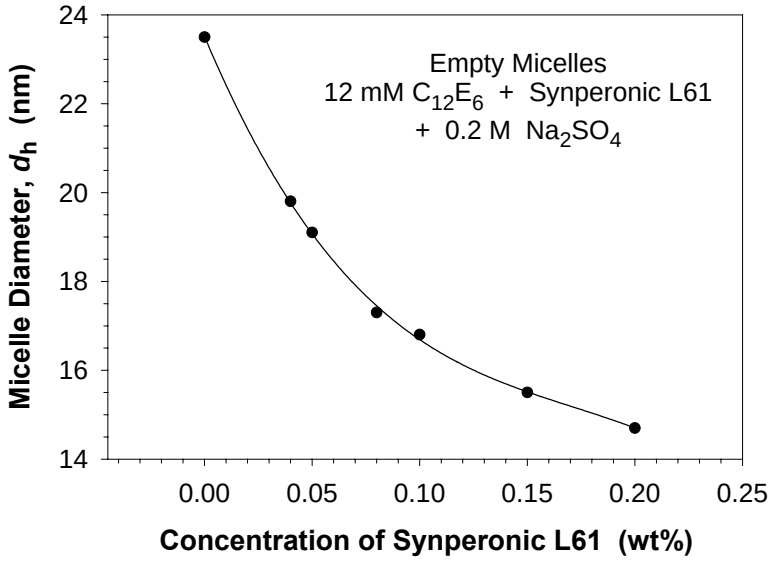

Figure 11. Hydrodynamic diameter d_h of the empty micelles vs. the concentration of SL61 for solutions containing (a) $C_{12}E_5$ and (b) $C_{12}E_6$. The continuous lines are fits by parabola.[17]

The biggest aggregates are formed in solutions of surfactant alone (without SL61 and solubilizate). Thus, for $C_{12}E_6$, the length of the rodlike micelles was $2b = 2pa \approx 88$ nm (see the last two columns of Table 2). The micelles of $C_{12}E_5$, alone, are even greater: they are known to form a network structure[64] and, consequently, their size cannot be determined by DLS. Upon addition of 0.1 wt % SL61 the $C_{12}E_5$ micelles become smaller and cylindrical, of length $2b \approx 134$ nm, which is still a considerable size

Table 2. Data for the mixed micelles of $C_{12}E_n$ + Synperonic L61 on triolein solubilization

Type of surfactant	SL61 [wt%]	$N_{surfact.}$	N_{SL61}	$N_{triolein}$	p	a [nm]
0 days (empty micelles)						
$C_{12}E_6$	0.0	1010	0	0	17.0	2.6
	0.1	518	22	0	11.5	2.4
	0.2	356	30	0	9.3	2.4
$C_{12}E_5$	0.1	1841	77	0	24	2.8
	0.2	895	74	0	21	2.4
	0.3	726	90	0	17	2.5
3 days						
$C_{12}E_6$	0.0	853	0	–	11.9	2.7
	0.1	252	11	6	3.7	2.8
	0.2	195	16	7	3.9	2.7
$C_{12}E_5$	0.1	729	30	26	8.0	3.0
	0.2	437	36	16	7.0	2.8
	0.3	331	41	12	6.5	2.7
10 days (full micelles)						
$C_{12}E_6$	0.0*	555*	0*	12*	4.8*	3.2*
	0.1	219	9	8	1.2	3.9
	0.2	198	16	9	2.6	3.1
$C_{12}E_5$	0.1	341	13	20	1	4.6
	0.2	261	22	15	1.3	4.1
	0.3	235	29	12	3.3	3.0

*After 16 days

Aggregation number and amount of solubilized oil. The main results from the SLS experiments are presented in Table 2 and Fig. 12. In general, we are dealing with large aggregates, which might contain hundreds of surfactant molecules and dozens of copolymer (SL61) molecules.

(a)

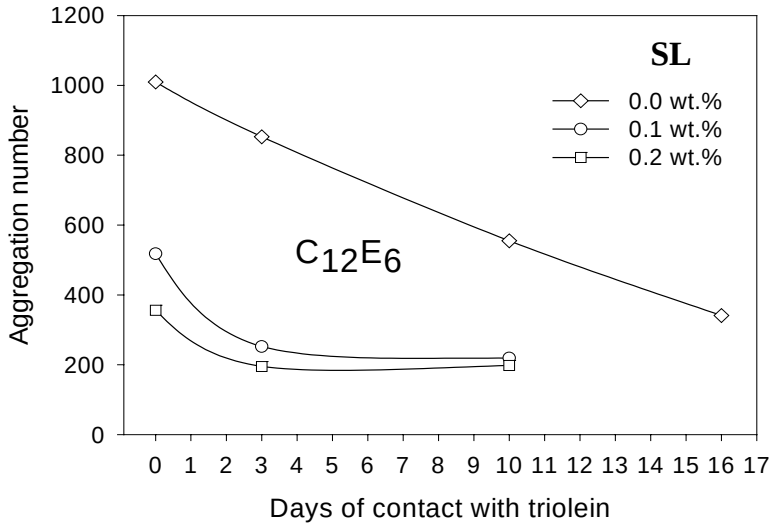

(b)

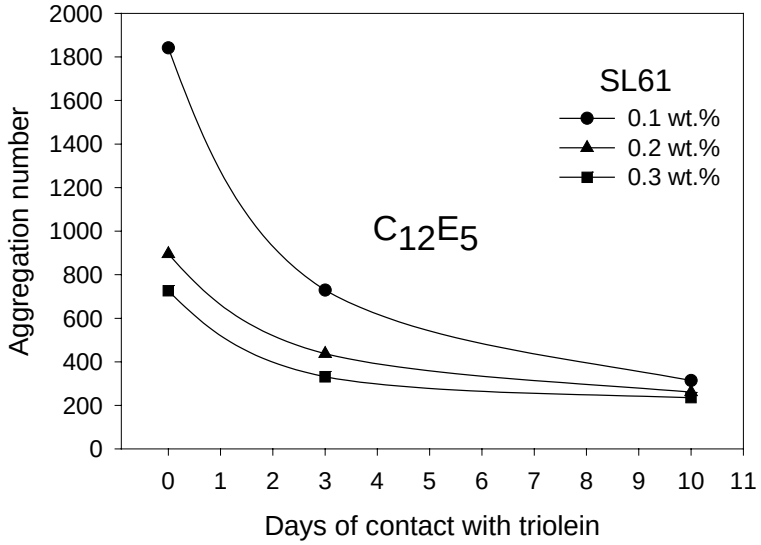

Figure 12. Variation of the micelle aggregation number, $N_{surfact}$, during the process of triolein solubilization in solutions of: (a) 12 mM $C_{12}E_5$ + 0.01 M NaCl, (b) 12 mM $C_{12}E_6$ + 0.2 M Na_2SO_4, in the presence of various concentrations of Synperonic L61 (SL61).[16]

In addition, the equilibrated swollen micelles (after 10 days, Table 2) contain between 8 and 20 solubilized triolein molecules per aggregate. As seen in Fig. 12, the micelles of $C_{12}E_5$ have larger aggregation number with respect to surfactant, $N_{surfact.}$, than those of $C_{12}E_6$, at equivalent other conditions. For the empty micelles (at zero days of contact in Fig. 12), $N_{surfact.}$

decreases with the rise of SL61 concentration (the micelles become smaller). During the process of solubilization, one observes a significant decrease of $N_{surfact.}$, especially during the first three days. The solubilization is faster for the solutions containing more SL61. Moreover, the solubilization is faster for the solutions of $C_{12}E_5$ in comparison with $C_{12}E_6$. Again, the changes in the solution of $C_{12}E_6$ *without* SL61 are the slowest (Fig. 12b).

Remarkably, the final ratio triolein/surfactant (after 10 days, Table 2) turns out to depend very slightly on the concentration of SL61 for a given nonionic surfactant: $N_{surfact.}/N_{triolein} \approx 17$ and 25 for $C_{12}E_5$ and $C_{12}E_6$, respectively. This result shows that the main role of SL61 is to accelerate the solubilization process, without affecting significantly the solubilization capacity of the micelles. The solubilization capacity of $C_{12}E_5$ is somewhat greater than that of $C_{12}E_6$ under these experimental conditions.

Shape of the micelles. As explained in section 4.2, the ellipsoidal shape of the micelles is described by two parameters: the length of the short semi-axis, a, and the ratio of the two semi-axes, $p = b/a$, see Fig. 10. The results from the calculations of these parameters are presented in Table 2 and Figs. 13 and 14. The length of the micelles decreases with the concentration of SL61 in the mixture (Fig. 13a). $C_{12}E_5$ forms about twice-longer micelles than $C_{12}E_6$ at the initial stages of solubilization (Fig. 13b).

In Table 2 and Fig. 14 one sees that the initial, strongly elongated empty micelles ($p \approx$ 9–24) transform into spheres ($p = 1$) or slightly deformed ellipsoids ($p \approx$ 2–3) as a consequence of the solubilization. The results about the change of the small semi-axis, a (Table 2), indicate that the change of the ratio $p = b/a$ is due mainly to shortening of the micelles: the increase of a is only about 50 to 70 % at the end of solubilization, whereas p decreases around 10 times. In other words, one empty micelle disintegrates into several smaller swollen micelles. From the ratio of the micelle aggregation numbers before and after solubilization, one can calculate the disintegration number, m, which enters the kinetic model in section 3.2. The overall picture of the micelle transformation upon solubilization is illustrated in Fig. 14.

The effect of the solubilized triolein on the size and shape of the investigated surfactant micelles resembles that of n-alkanes. Therefore, one may expect that the triglycerides are incorporated preferentially inside the hydrophobic core of the micellar aggregates.[16]

(a)

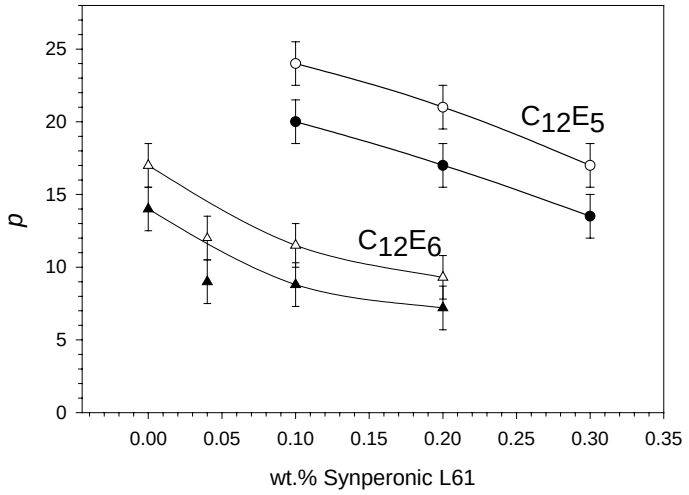

(b)

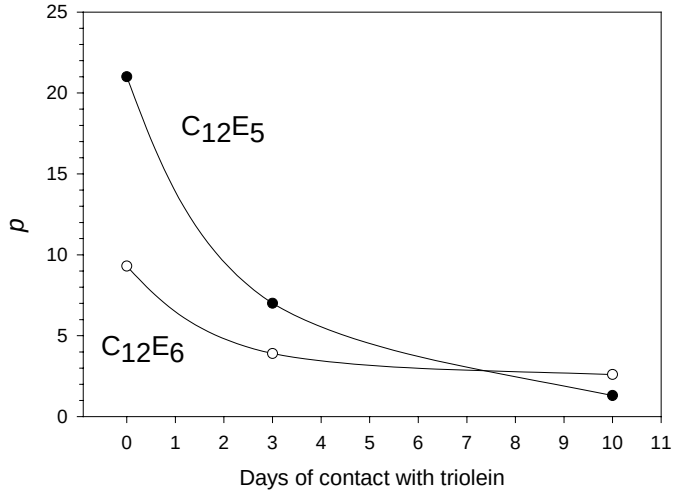

Figure 13. (a) Aspect ratio $p = b/a$ of ellipsoidal empty micelles vs. the concentration of SL61; p is calculated assuming that either 2 or 4 water molecules per ethoxy group are present (the solid and empty symbols, respectively). (b) Variation of p during the process of triolein solubilization at fixed 0.2 wt % SL61. The surfactant concentration is 12 mM $C_{12}E_n$; the inorganic salts are as in Fig. 11.[16]

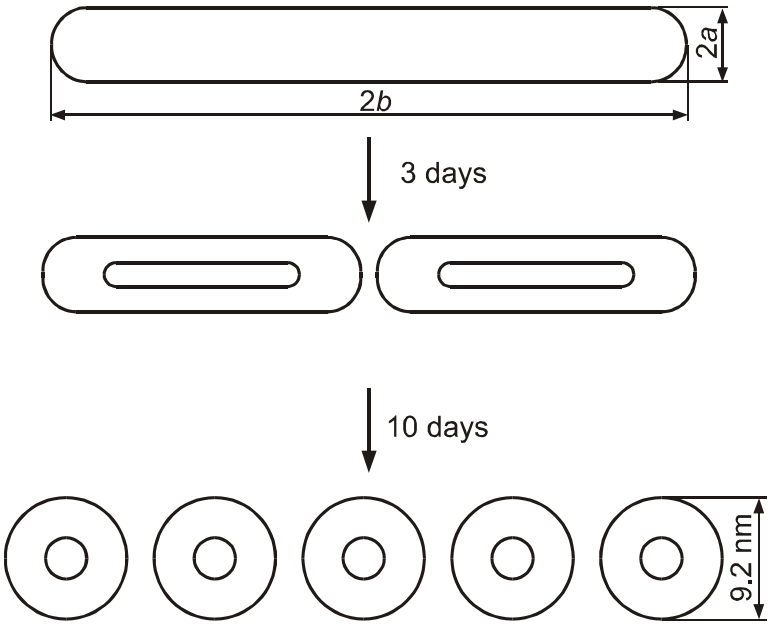

Figure 14. Sketch of the changes in the average micelle size and shape during the solubilization in a solution of 12 mM $C_{12}E_5$ + 0.1 wt % SL61 + 0.01 M NaCl. The ratio of the long to the short semi-axes is drawn to the real scale.[16]

5. Nonionic surfactants in mixture with triblock copolymers: Solubilization kinetics

5.1. Experimental results

Table 3 summarizes our results[18] for the solubilization of triolein drops in micellar solutions of $C_{12}E_5$ and $C_{12}E_6$ at several concentrations of added SL61. The first column shows the concentration of SL61. The values of m (the number of swollen micelles obtained by splitting of an empty micelle upon solubilization) are obtained by analysis of the static light-scattering data (Table 2). The solubilization kinetic parameters α and β are determined as adjustable parameters from the best fit of data for diminishing oil drops (like those in Fig. 9) by means of Eq [39]. Next, the compound solubilization rate constant, χ, and the number of triolein molecules per swollen micelle, n_s, are calculated from the respective values of α and β by using Eq [40] and data for D_1 and c_{10} in Table 1. For comparison, the last column of Table 3 contains values of n_s, which have been obtained in an independent way, by means of NMR spectroscopy in combination with static light scattering; for details see Ref 16. Note that the parameters m and n_s [NMR] are obtained in *equilibrium* experiments (triolein phase

equilibrated with the micellar solution), whereas the parameters α and β are determined in *kinetic* experiments with separate diminishing triolein drops in the cell from Fig. 3.

Table 3. Equilibrium and kinetic parameters related to the solubilization of triolein drops

C_{SL61} [wt %]	m	α [nm/s]	$\beta \times 10^6$ [s^{-1}]	χ (μm/s) (Eq. 40)	n_s (Eq. 40)	n_s (NMR)
(a) Solutions of 0.012 M $C_{12}E_5$ + 0.01 M NaCl						
0.0	–	0.14 ± 0.01	3 ± 1	0.20	–	–
0.1	5.4	0.21 ± 0.01	4.7 ± 1	0.34	20	20 ± 3
0.2	3.5	0.68 ± 0.03	37 ± 5	1.05	16	15 ± 2
0.3	3.1	1.05 ± 0.07	85 ± 14	1.74	13	12 ± 2
(b) Solutions of 0.012 M $C_{12}E_6$ + 0.2 M Na_2SO_4						
0.0	3.0	0.034 ± 0.01	0.34 ± 0.06	0.22	5	12 ± 2
0.05	2.7	0.33 ± 0.02	17 ± 3	1.40	6	10 ± 2
0.1	2.4	0.47 ± 0.03	22 ± 4	1.44	7	8 ± 1
0.2	1.8	0.53 ± 0.03	22 ± 4	1.43	7	9 ± 1

5.2. Discussion

As a characteristic of the solubilization rate we can use the kinetic parameter α, which is independent of the drop size, see Eqs [36] and [37]. In fact, $\alpha = |dR/dt|$ for sufficiently small drops, that is in the limiting case $(\beta/\alpha)R << 1$, see Eq [36]. Accepting α as a measure of the solubilization rate, from Table 3 we can conclude that the addition of SL61 to the solutions of nonionic surfactants strongly accelerates the solubilization. For example, the addition of 0.2 wt % SL61 increases the solubilization rate of triolein in the investigated solutions of $C_{12}E_5$ and $C_{12}E_6$, respectively, 5 and 15 times.

The compound solubilization kinetic constant χ also exhibits a tendency to increase with the rise of the SL61 concentration (Table 3). According to Eq [34], this parameter can be expressed in the form

$$\chi \equiv \frac{k_{1,a}}{1 + k_{1,d}/k_s} \qquad [49]$$

where $k_{1,a}$ and $k_{1,d}$ are the rate constants of adsorption and desorption of empty micelles at the oil-water interface, and k_s is the rate constant of the uptake of oil, that is of the reaction given

by Eq [22]. If the latter reaction is sufficiently fast, i.e. if $k_s >> k_{1,d}$, then Eq [49] predicts $\chi \approx k_{1,a}$, which means that the total solubilization rate is limited by the rate of adsorption of the empty micelles. If this is the case, all adsorbed empty micelles will be completely transformed into 'equilibrated' swollen micelles, before their desorption (insofar as $k_s >> k_{1,d}$). The coincidence of the data for n_s in the last two columns of Table 3a indicates that this is really the case for the investigated solutions of $C_{12}E_5$. Indeed, Eq [40] gives a kinetic value of n_s, determined from the time dependence, $R(t)$, of the radius of diminishing oil drops, see Fig. 9. On the other hand, the value of n_s obtained by means of NMR refers to micellar solutions, which have been equilibrated with the oil phase. Moreover, the good agreement between the data for n_s in the last two columns of Table 3a is an argument in favour of the correctness of our theoretical interpretation of the light-scattering data about the mixed micelles, as well as of the data for diminishing oil drops obtained in the capillary cell (Fig. 3).

The rate constant of micelle adsorption can be expressed in the form $k_{1,a} = P\exp(-E_a/kT)$, where P is a pre-exponential factor and E_a is the activation energy; that is the empty micelles encounter a barrier to adsorption of height E_a. For the studied $C_{12}E_5$ solutions, it turns out that the magnitude of E_a controls the solubilization rate. Our model considerations in Ref 17 showed that the height of the adsorption barrier is proportional to the length L of the rodlike micelles, that is, $E_a = wL$, where w is the activation energy per unit length of the rodlike micelle. Therefore, one may expect that

$$\ln(\chi) \approx \ln(k_{1,a}) \approx A_1 - \frac{w}{kT} L \qquad [50]$$

where A_1 and w are (in first approximation) constant parameters. To check whether our data complies with Eq [50], in Fig. 15 we have plotted $\ln(\chi)$ vs. L; the values of χ are from Table 3a for $C_{SL61} = 0.1$, 0.2 and 0.3 wt %; the length of the empty micelles, $L = 2pa$, was computed using the values of p and a from Table 2. Figure 15 shows that our data do agree with Eq [50]. The slope yields $w = 0.034\ kT$ per nm. Thus for micelles of length $L = 50$, 100 and 150 nm, the estimated height of the adsorption barrier is $E_a = 1.7$, 3.4 and 5.1 kT, respectively.[18]

The agreement of our data with Eq [50] (Figure 15) implies that the addition of SL61 to the solution of nonionic surfactant decreases the length of the rodlike micelles, thus reducing the kinetic barrier to adsorption and accelerating the solubilization process. However, this is not the only way SL61 affects the solubilization rate. As mentioned earlier, the latter is characterized by the kinetic parameter $\alpha = \lambda v_0 m n_s \chi c_{10}$. The addition of SL61, at

fixed concentration of $C_{12}E_n$, simultaneously increases χ and c_{10}, but decreases m and n_s (see Table 3). In a final reckoning, the growth of the product $\chi\, c_{10}$ prevails and determines the overall increase of α with the rise of the SL61 concentration.

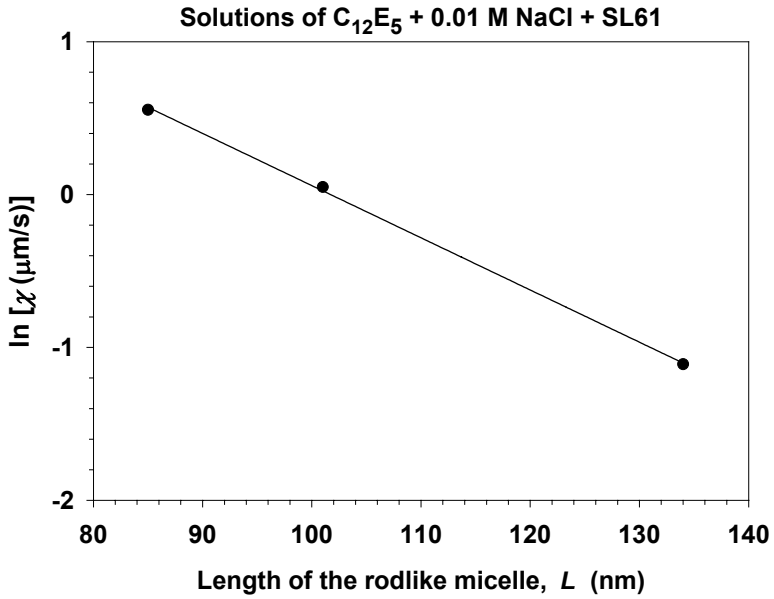

Figure 15. Plot of data from Table 3a for the compound solubilization rate constant, χ, vs. the length, L, of the rodlike micelles, in accordance with Eq [50].[18]

In the case of $C_{12}E_6$, the solubilization rate α also increases with the rise of the SL61 concentration, see Table 3b. In this case the kinetic values of n_s are systematically lower than the equilibrium values of n_s determined by NMR (cf. the last two columns of Table 3b), the difference being larger for the lower concentrations of SL61. A possible explanation is the following.

Kinetic values of n_s, lower than the equilibrium ones, imply that the micelles may prematurely desorb from the oil-water interface, before the completion of the reaction, Eq [22], i.e. before taking the maximal possible number of oil molecules per micelle. In view of Eq [49], this means that the rate constants of desorption and solubilization are comparable, that is the ratio $k_{1,d}/k_s$ is not much smaller than 1. Such a behaviour could be attributed to the fact that the hydrophilic polyoxyethylene brushes of the adsorption layers (and micelles) from $C_{12}E_6$ are thicker and more hydrated than those from $C_{12}E_5$. Thus, the transport of a hydrophobic triolein molecule from the oil phase, across the hydrophilic brush, into the core of an adsorbed micelle, encounters a higher kinetic barrier (smaller k_s) in the case of $C_{12}E_6$. In addition, a more hydrophilic brush implies a weaker adhesion of the micelles to the oil-water

interface, that is a greater desorption rate constant $k_{1,d}$. Both effects tend to increase the ratio $k_{1,d}/k_s$ for $C_{12}E_6$, in comparison with $C_{12}E_5$. The addition of SL61 seems to make the micelles and the adsorption layers more hydrophobic (that is more "sticky"), which decreases the ratio $k_{1,d}/k_s$. This is indicated by the closer kinetic and equilibrium values of n_s for the higher concentrations of SL61 in Table 3b. The markedly strong increase of the solubilization rate with the rise of C_{SL61} (more than 15 times) in the case of $C_{12}E_6$, seems to be a manifestation of this "hydrophobizing action" of Synperonic L61.

6. Ionic surfactants in mixture with triblock copolymers: Solubilization kinetics

6.1. Solubilization in the absence of copolymer

As discussed above, the solubilization of triglycerides by nonionic surfactant solutions occurs through a transient attachment of micelles to the oil-water interface. Then, every factor that impedes the micelle adsorption, would lead to suppression of the process, or to its complete ceasing. As discussed by Chen et al.,[14] such a factor is the electrostatic repulsion between the micelles and the oil-water interface, the latter being covered with a surfactant adsorption monolayer, which bears electric charges having the same sign as the charge of the micelles.

To examine the effect of electrostatic repulsion, we added various portions of the anionic surfactant sodium dodecyl-dioxyethylene sulfate (SDP2S) to the solution of 12 mM $C_{12}E_6$ + 0.2 M Na_2SO_4. Thus the molar fraction of SDP2S in the surfactant blend,

$$X_{SDP2S} = C_{SDP2S}/(C_{C12E6} + C_{SDP2S}), \qquad [51]$$

was varied (C denotes molar concentration). The addition of SDP2S to the $C_{12}E_6$ solutions does not significantly affect the micelle size: by means of dynamic light scattering (DLS; Malvern 4700C, UK) we found that the hydrodynamic diameter of the empty micelles varies within 10 % for $0 \le X_{SDP2S} \le 0.25$.

Figure 16 shows the rate of solubilization of soybean oil, characterized by $|dR/dt|$, as a function of X_{SDP2S}. The results demonstrate that the solubilization rate considerably decreases for $X_{SDP2S} \ge 0.10$; furthermore, the solubilization is completely ceased for $X_{SDP2S} \ge 0.17$. These findings can be attributed to a growth of the electrostatic barrier to micelle adsorption and to a decrease in the respective adsorption energy, caused by the rise of the negative surface electric charge. Our results are consonant with the findings of other authors[14,68-70] that

the solubilization is suppressed in the presence of ionic surfactants, except in the case of oils, which exhibit a considerable solubility in pure water.[8]

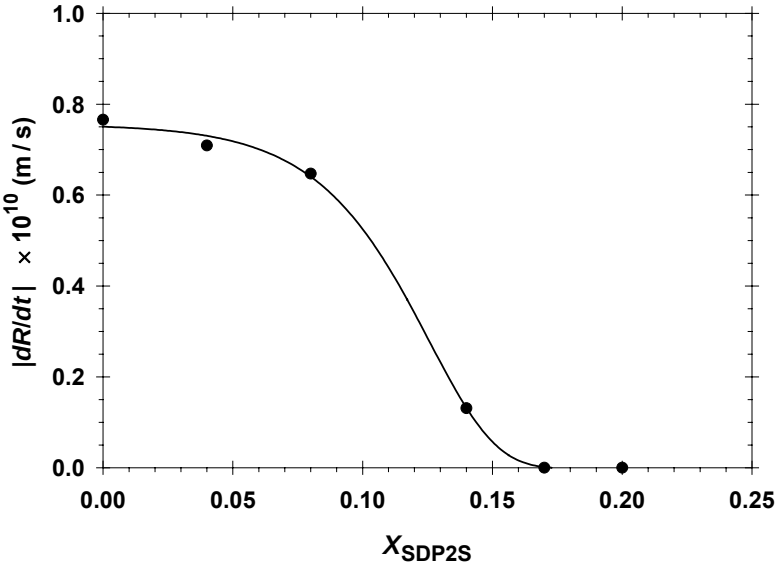

Figure 16. Rate of solubilization of soybean oil vs. the mole fraction of SDP2S in mixture with $C_{12}E_6$; all solutions contain 12 mM $C_{12}E_6$ and 0.2 M Na_2SO_4. The experiments are carried out with separate oil drops of initial radius $R_0 \approx 35$ μm with the cell in Fig. 5.[18]

On the other hand, ionic surfactants are most frequently involved in detergency formulations because of their useful properties. One way to put down their inhibitory action on solubilization is to reduce the electrostatic barrier by addition of some divalent or trivalent counterions, as discussed below.

Large rod-like micelles are formed in solutions of anionic surfactants in the presence of inorganic electrolytes, and especially of salts with divalent and trivalent counterions.[71,72] In Ref 72 it has been shown that the binding of Al^{3+} to the SDP2S headgroups essentially reduces the micelle negative surface charge and gives rise to the formation of long rodlike micelles. Moreover, one could hypothesize that the Al^{3+} ions might bridge between the micelle and the oil-water interface and to bring about micelle adsorption. To check whether such micelles are able to solubilize triglycerides, we carried out experiments on solubilization of triolein in solutions of SDP2S in the presence of Al^{3+} counterions. However, our experiments with this system (the system SDP2S + Al^{3+}) showed that triolein is not solubilized in such anionic micellar solutions. The reasons for the latter negative result could be at least two: (i) Despite the binding of Al^{3+}, the electrostatic repulsion remains large

enough to prevent the micelle adsorption at the oil-water interface; (ii) even if micellar adsorption takes place, the water-rich film, intervening between micelle and oil, may create a high kinetic barrier to the transfer of hydrophobic triglyceride molecules from the oil phase into the micelle. Further experiments showed[73] that the problem can be resolved if a triblock copolymer, such as Synperonic L61 (SL61), is added to this system.

6.2. Solubilization in the presence of copolymer and trivalent counterions

As explained in the previous subsection, in the absence of SL61, the solutions of SDP2S + $AlCl_3$ do not solubilize triolein. Then, a basic question appears: whether the inability of ionic surfactants to solubilize triglycerides is due to *kinetic* factors (high micelle adsorption barrier, or barrier to the transfer of oil), or to *thermodynamic* factors. The occurrence of solubilization, when SL61 is added to the solution of SDP2S + $AlCl_3$, indicates that the reason is kinetic, rather than thermodynamic. The analysis of the experimental data from the solubilization kinetics implies that the kinetic (electrostatic) barrier is suppressed only in the presence of both SL61 and $AlCl_3$. In particular, the addition of $AlCl_3$ to the SDP2S solutions leads to binding of Al^{3+} counterions at the micelle and oil-drop surfaces, thus reducing the negative surface potential and the adsorption barrier per unit length of the micelle. However, the Al^{3+} counterions induce the growth of long rodlike micelles of SDP2S. As the adsorption barrier is proportional to the micelle length, the SDSP2S micelles in the presence of $AlCl_3$ turn out to be too long to overcome the barrier and, consequently, they do not adsorb at the oil-drop surface. The addition of SL61 leads to a decrease in the micelle length, thus reducing the adsorption barrier and promoting the solubilization by the mixed SDP2S/SL61 micelles.[73]

In summary, Al^{3+} promotes the solubilization by reducing the micelle surface charge, while SL61 promotes the solubilization by decreasing the length of the rodlike micelles. Our further analysis of the data for the system SDP2S + SL61 +Al^{3+} showed the existence of three main differences with the system {nonionic} + SL61, considered in section 5:

First, in the presence of SL61, the empty and swollen micelles of SDP2S are relatively small: spherical or slightly elongated. Such small aggregates do not break down to smaller micelles upon solubilization (as it is with the long rodlike micelles of EO5 and EO6 considered in section 5).

Second, we observed that the oil drops in emulsions containing SDP2S + SL61 +Al^{3+} are sticky: they adhere to each other and to the walls of the vessel. As the composition of the adsorption layer on the drop surface and of the micelles is similar, one can expect that the micelles in this system are also sticky. The latter implies a higher coverage of the oil-drop surface with adherent micelles. Consequently, one might expect that the micelle adsorption can be beyond the linear Henry region of the adsorption isotherm. In other words, the simple Henry isotherm, used by us to interpret the data for EO5 and EO6 in section 5, is not applicable in the present case. For that reason, for the system SDP2S + SL61 +Al^{3+}, we used the Langmuir isotherm to describe the adsorption of micelles at the oil-water interface.

Third, since the uptake of oil is expected to render the micelles more hydrophobic, the rate constants of adsorption and desorption can be, in general, different for the empty and swollen micelles. As before, we use subscripts '1' and '2' to denote, respectively, empty and swollen micelles. Thus, we arrive at a kinetic model with two micelle-*adsorption* rate constants, k_{1a} and k_{2a}, two micelle-*desorption* rate constants, k_{1d} and k_{2d}, and one rate constant of solubilization (uptake of oil by the empty micelles), k_s.

Because the experimental system and conditions are different (as compared to the case of nonionic surfactants), in Ref 73 we arrived at a kinetic model, which is different from that in section 3.2. The comparison of the new model against experimental data for ionic surfactants (+ SL61) showed that $k_s >> k_{1d}$, and $k_{2a} >> k_{1a}$. The latter relationship means that the adsorption is faster for swollen micelles, than for empty micelles. In other words, the barrier to adsorption of swollen micelles is lower. Under these circumstances, the theory[73] provides the following approximate expression for the dependence $R(t)$:

$$\frac{dR^{3/2}}{dt} \approx -\frac{3D_1 c_{10} \lambda n_s \mathrm{v}_0}{2l^{1/2}} \equiv S_\mathrm{r} = \text{const.} \qquad [52]$$

$$l = A_\infty D_1 c_{10} \frac{k_{2a}}{k_{1a} k_{2d}} \qquad [53]$$

where A_∞ is the excluded area per adsorbed micelle, and the constant (independent of drop size) parameter S_r characterizes the *solubilization rate*.

In accordance with Eq [52], we plotted the experimental data for the system SDP2S + SL61 + Al^{3+} as $R^{3/2}$ vs. t. The data were found to agree very well with Eq [52], see Fig. 17.

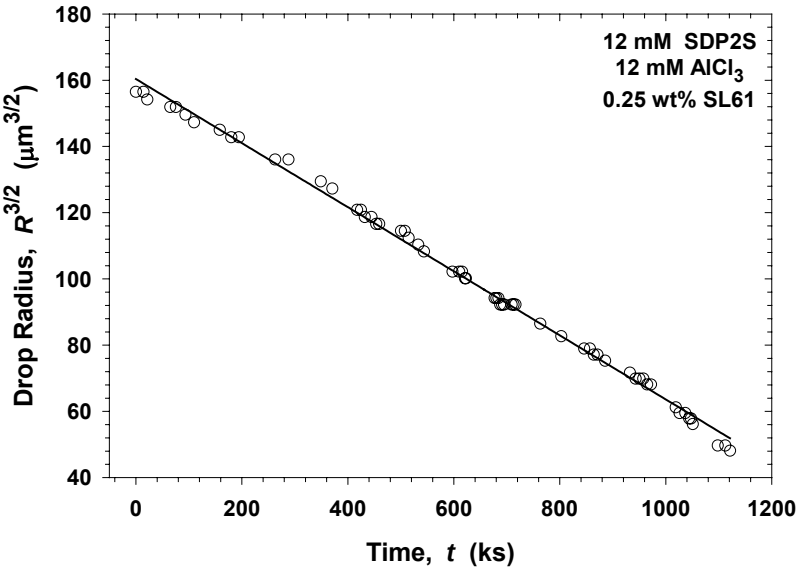

Figure 17. Plot of $R^{3/2}$ vs. time, t (1 ks = 1000 s), for a triolein drop subjected to solubilization in micellar solutions of 12 mM SDP2S + 12 mM $AlCl_3$, containing also 0.25 wt% SL61. The symbols are experimental points; the line is the best fit by means of Eq [52].[73]

From the slope of lines, like that in Fig. 17, the parameters l and S_r were determined - see Table 4. As seen from the table, S_r increases with the addition of SL61, i.e. SL61 accelerates the solubilization of triolein for this system.[73]

Table 4. Parameters related to the solubilization of triolein in solution containing 12 mM SDP2S + 12 mM $AlCl_3$ at various concentrations of SL61.

C_{SL61} [wt %]	D_1 [10^{-7} cm^2/s]	c_{10} [10^{16} cm^{-3}]	n_s (NMR)	l [mm]	S_r [μm$^{3/2}$/(ks)]
0.25	5.54	4.42	5	73.4	0.01
0.50	6.38	8.67	4	4.27	0.74
0.75	5.81	10.4	4	4.39	0.80
1.00	5.44	11.4	4	1.30	1.51

Figure 18 shows similar data for the solubilization of separate triolein drops in micellar solutions of the anionic surfactant sodium dodecylbenzene sulfonate (DDBS). The addition of 12 mM $AlCl_3$ led to precipitation of the DDBS solutions. To avoid precipitation, we added Triton X-100 to the surfactant solutions. Thus, the system becomes DDBS + Triton X-100 + SL61 + Al^{3+}. Again, solubilization of triolein takes place only if SL61 and Al^{3+} are simultaneously present. The three almost parallel lines in Fig. 18 correspond to three

diminishing triolein drops.[73] The data illustrates how reproducible is the value of the solubilization rate parameter, S_r, determined from the slope of the different lines.

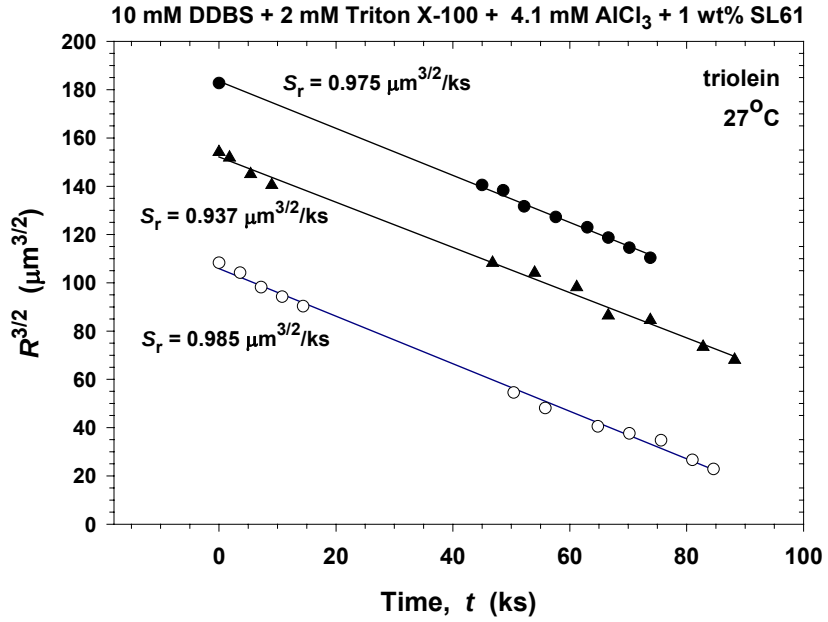

Figure 18. Plots of $R^{3/2}$ vs. time, t, for three triolein drops subjected to solubilization in micellar solutions of 10 mM DDBS + 2 mM Triton X-100 + 4.1 mM $AlCl_3$, containing also 1 wt% SL61. The symbols are experimental points; the lines are the best fits by means of Eq [52].[73]

If the crucial factor, governing the solubilization kinetics, is the electrostatic barrier to micelle adsorption at the oil-water interface (as implied by our data analysis), then one could expect that a mere change of the sign of the electric charges should not alter the overall occurrence of the solubilization process. To check that, we made the following changes in the solubilization system: (i) the *anionic* surfactant (SDP2S, DDBS) was replaced with a *cationic* surfactant, dodecyl trimethyl ammonium bromide (DTAB) or hexadecyl trimethyl ammonium bromide (HTAB). (ii) The *positive* trivalent counterion (Al^{3+}) was replaced with a *negative* one ($Citrate^{3-}$). Figure 19 shows that solubilization of triolein takes place again and that the solubilization rate (characterized by S_r) is comparable with that for anionic surfactants (cf. Table 4 and Figs. 17 and 18). The solubilization rate for HTAB is about 2 times greater than that for DTAB (all other conditions the same), which is indicated by the greater slope of the line for HTAB in Fig. 19. For the investigated concentration range, we found[73] that if the concentration of SL61 is increased 3 times, S_r increases by a factor of 12.5.

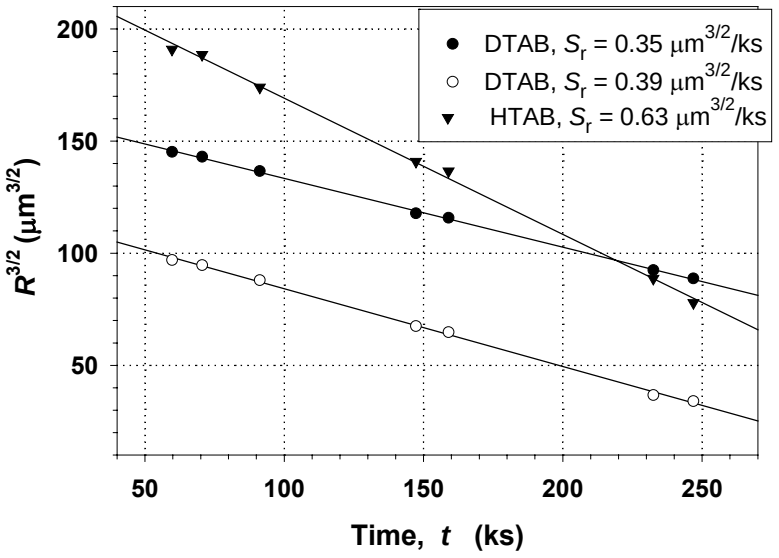

Figure 19. Plots of $R^{3/2}$ vs. time, t, for three triolein drops subjected to solubilization. The used micellar solutions contain 12 mM DTAB or 12 mM HTAB, as well as 0.1 M Na_3Citrate and 1 wt% SL61. The symbols are experimental points; the lines are the best fits by means of Eq [52].[73]

7. Conclusions and future trends

The solubilization could happen as either bulk or surface reaction (Figs. 1 and 2).

The case of bulk reaction is typical for oils that exhibit a pronounced solubility in water. By experiments with single drops (Fig. 3) one can determine the kinetic parameters of the process: the mass transfer coefficient of oil across the oil-water interface, α_0, and the rate constant of solubilization, k_+; see section 3.1. The data for solubilization of decane by SDS micelles indicate that the act of catching of an oil molecule by a micelle occurs under a barrier (rather than diffusion) control.

The case of surface reaction is typical for oils that have negligible solubility in water. In the practically important case of triglycerides, we found that solubilization may happen in mixed solutions of nonionic surfactant ($C_{12}E_5$ and $C_{12}E_6$) and triblock copolymer (Synperonic L61). The mixed micelles in these solutions contain hundreds to thousand surfactant molecules and dozens of polymer (SL61) molecules; see section 4. The developed theoretical model (section 3.2) and its comparison with the experiment (section 5) allowed us to determine the compound rate constant of solubilization, $\chi \approx k_a$, and the number of oil molecules in a swollen micelle, n_s.

The addition of SL61 to the micellar solutions of $C_{12}E_5$ and $C_{12}E_6$ leads to a considerable decrease in the average micelles size (Fig. 11 and Table 2). In this way, SL61 promotes solubilization by decreasing the barrier to micelles adsorption at the oil-water interface: this barrier is proportional to the length of the rodlike micelles; see Eq [50] and Fig. 15.

The ionic surfactants are unable to solubilize triglycerides, because the strong electrostatic repulsion between the micelles and the oil-water interface prevents them from coming into contact. This kinetic barrier can be suppressed by simultaneous addition of triblock copolymer (SL61) and trivalent counterions (Al^{3+} for anionic surfactant and $Citrate^{3-}$ for cationic surfactant); see section 6. The binding of counterions reduces the surface electric charge of the rodlike micelles, but increases their length. In its own turn, the addition of SL61 decreases the average micelle length and reduces the barrier to micelle adsorption at the oil-water interface. Hence, the triblock copolymer again acts as a promoter of solubilization.

In the present chapter, we demonstrated that different kinetic mechanisms could be realized for different experimental systems. The developed theoretical models have been successfully tested against experimental data. A question, which is still open, is how general are these models, i.e. whether some other mechanisms could exist for other systems. Possible trends for the future studies follow also from the novelty of the presented results. At our best knowledge, the data in section 6 are the first results for solubilization of triglycerides by solutions of *ionic* surfactants. The types of block copolymers, electrolytes and surfactants, as well as the working concentrations, are far from being completely investigated and optimised. We hope that the conclusions about the specific kinetic mechanisms of solubilization, presented in this chapter, and the related theoretical models, will be helpful for a future development in this field.

Acknowledgements. This work was sponsored by Colgate-Palmolive. The authors acknowledge the valuable contributions of their colleagues, Prof. K. Danov, Dr. R. Alargova, Dr. G. Marinov, Mrs. S. Kralchevska, Mr. P. Todorov and Mr. N. Christov, to the research papers reviewed in the present chapter.

References

1 McBain J W, *Colloidal Science*, Lexington, Mass., D C Heat, 1950.

2 Christian S D, Scamehorn J F, *Solubilization in Surfactant Aggregates*, New York, M Dekker, 1995.

3 Miller C A, 'Micellar systems and microemulsions', in Birdi K S, *Handbook of Surface and Colloid Chemistry* (1st Edition), Boca Raton, CRC Press, 1997; 157-178.

4 Vasilescu M, Caragheorgheopol A, Caldararu H, 'Aggregation numbers and microstructure characterization of self-assembled aggregation of poly(ethylene oxide) surfactants and related block-copolymers, studies by spectroscopic methods', *Adv. Colloid Interface Sci.* 2001 **89-90**(1) 169-194.

5 Carroll B J, 'The kinetics of solubilization of nonpolar oils by nonionic surfactant solutions', *J. Colloid Interface Sci.* 1981 **79**(1) 126-135.

6 Kabalnov A, Weers J, 'Kinetics of mass transfer in micellar systems: surfactant adsorption, solubilization kinetics and ripening', *Langmuir* 1996 **12**(14) 3442-3448.

7 Weiss J, Coupland J N, Brathwaite D, McClements D J, 'Influence of molecular structure of hydrocarbon emulsion droplets on their solubilization in nonionic surfactant micelles', *Colloids Surf. A* 1997 **121**(1) 53-60.

8 Todorov P D, Kralchevsky P A, Denkov N D, Broze G, Mehreteab A, 'Kinetics of solubilization of *n*-decane and benzene by micellar solutions of sodium dodecyl sulfate'**,** *J. Colloid Interface Sci.* 2002 **245**(2) 371-382.

9 Sailaja D, Suhasini K L, Kumar S, Gandhi K S, 'Theory of rate of solubilization into surfactant solutions', *Langmuir* 2003 **19**(9) 4014-4026.

10 Chan A F, Fennel Evans D, Cussler E L, 'Explaining solubilization kinetics', *AIChE J.* 1976 **22**(6) 1006-1012.

11 Huang C, Fennel Evans D, Cussler E L, 'Linoleic acid solubilization with a spinning liquid disc', *J. Colloid Interface Sci.* 1981 **82**(2) 499-506.

12 Shaeiwitz, J. A.; Chan, A. F.-C.; Cussler, E. L.; Fennel Evans, D, 'The Mechanism of solubilization in detergent solutions', *J. Colloid Interface Sci.* 1981 **84**(1) 47-56.

13 Plucinski P, Nitsch W, 'Kinetics of interfacial phenylalanine solubilization in a liquid/liquid microemulsion system', *J. Phys. Chem.* 1993 **97**(35) 8983-8988.

14 Chen B-H, Miller C A, Garrett P R, 'Rates of solubilization of triolein into nonionic surfactant solutions', *Colloids Surf. A* 1997 **128**(1) 129-143.

15 Chen B-H, Miller C A, Garrett P R, 'Rates of solubilization of triolein/fatty acid mixtures by nonionic surfactant solutions', *Langmuir* 1998 **14**(1) 31-41.

16 Christov N C, Denkov N D, Kralchevsky P A, Broze G, Mehreteab A, 'Kinetics of triglyceride solubilization by micellar solutions of nonionic surfactant and triblock copolymer: 1. The empty and swollen micelles', *Langmuir* 2002 **18**(21) 7880-7886.

17 Kralchevsky P A, Denkov N D, Todorov P D, Marinov G S, Broze G, Mehreteab A, 'Kinetics of triglyceride solubilization by micellar solutions of nonionic surfactant and triblock copolymer: 2. Theoretical model', *Langmuir* 2002 **18**(21) 7887-7895.

18 Todorov P D, Marinov G S, Kralchevsky P A, Denkov N D, Durbut P, Broze G, Mehreteab A, 'Kinetics of triglyceride solubilization by micellar solutions of nonionic surfactant and triblock copolymer: 3. Experiments with single drops', *Langmuir* 2002 **18**(21) 7896-7905.

19 Granek R, 'Spontaneous curvature-induced Rayleigh-like instability in swollen cylindrical micelles', *Langmuir* 1996 **12**(21) 5022-5027.

20 Lawrence A S C, 'Solubility in soap solutions. Part 10: Phase equilibrium, structural and diffusion phenomena involving the ternary liquid crystalline phase', *Discuss. Faraday Soc.* 1958 **25**(1) 51-58.

21 Lawrence A S C, Bingham A, Capper C B, Hume K, 'The penetration of water and aqueous soap solutions into fatty substances containing one or two polar groups', *J. Phys. Chem.* 1964 **68**(12) 3470-3476.

22 Stowe L R, Shaeiwitz J A, 'Liquid solubilization dynamics: oleic acid in bile salt', *J. Colloid Interface Sci.* 1982 **90**(2) 495-508.

23 Raterman, K T, Shaeiwitz J A, 'Liquid solubilization dynamics. II. Flux enhancement by interface gel formation', *J. Colloid Interface Sci.* 1984 **98**(2) 394-404.

24 Lim J-C, Miller C A, Dynamic behavior and detergency in systems containing nonionic surfactants and mixtures of polar and nonpolar oils', *Langmuir* 1991 **7**(10) 2021-2027.

25 Somasundaran P, Krishnakumar S, 'Adsorption of surfactants and polymers at the solid-liquid interface', *Colloids Surf. A* 1997 **123-124**(1) 491-513.

26 Ward A J, 'Kinetics of solubilization in surfactant-based systems', in Christian S D, and Scamehorn J F, *Solubilization in Surfactant Aggregates*, New York, Dekker M, 1995; Chapter 7.

27 Nagarajan R, Ganesh K, 'Comparison of solubilization of hydrocarbons in (PEO-PPO) diblock versus (PEO-PPO-PEO) triblock copolymer micelles', *J. Colloid Interface Sci.* 1996 **184**(2) 489-499.

28 Lebens P J M, Keurentjes J T F, 'Temperature-induced solubilization of hydrocarbons in aqueous block copolymer solutions', *Ind. Eng. Chem. Res.* 1996 **35**(10) 3415-3421.

29 Xing L, and Mattice W L, 'Strong solubilization of small molecules by triblock-copolymer micelles in selective solvents', *Macromolecules* 1997 **30**(6) 1711-1717.

30 Kříž J, Masař B, Doskočilová D, 'NMR studies of the structure and interactions of block copolymer micelles in water. 4. Diffusion of organic solubilizates into the micellar core', *Macromolecules* 1997 **30**(15) 4391-4397.

31 Marinov G, Michels B, Zana R, 'Study of the state of the triblock copolymer poly (ethylene oxide)–poly (propylene oxide)–poly (ethylene oxide) L64 in aqueous solution', *Langmuir* 1998 **14**(10) 2639-2644.

32 Kositza M J, Bohne C, Alexandridis P, T. Hatton T A, Holzwarth J F, 'Micellization dynamics and impurity solubilization of the block-copolymer L64 in an aqueous solution' *Langmuir* 1999 **15**(2) 322-325.

33 Walderhaug H, 'PFG NMR study of polymer and solubilizate dynamics in aqueous isotropic mesophases of some poloxamers', *J. Phys. Chem. B* (1999) **103**(17) 3352-3357.

34 Paterson I F, Chowdhry B Z, Leharne S A, 'Investigations of naphthalene solubilization in aqueous solutions of ethylene oxide-*b*-propylene oxide-*b*-ethylene oxide copolymer', *Langmuir* 1999 **15**(19) 6187-6194.

35 Bromberg L, Temchenko M, 'Solubilization of hydrophobic compounds by micellar solutions of hydrophobically modified polyelectrolytes', *Langmuir* 1999 **15**(25) 8627-8632.

36 Chiu Y C, Chang C Y, 'Factors affecting the solubilization of hydrocarbon in polyoxyethylene mono *n*-dodecylether', *J. Surface Sci. Technol.* 1990 **6**(4) 349-368.

37 Prak D J L, Abriola L M, Weber Jr. W J, Bocskay K A, Pennell K D, Solubilization rates of *n*-alkanes in micellar solutions of nonionic surfactants', *Environ. Sci. Technol.* 2000 **34**(3) 476-482.

38 McClements D J, Dungan S R, 'Light scattering study of solubilization of emulsion droplets by non-ionic surfactant solutions', *Colloids Surf. A* 1995 **104**(1) 127-135.

39 Coupland J N, Brathwaite D, Fairley P, McClements D J, 'Effect of ethanol on the solubilization of hydrocarbon emulsion droplets in nonionic surfactant micelles', *J. Colloid Interface Sci.* 1997 **190**(1) 71-75.

40 Carroll B J, 'The accurate measurement of contact angle, phase contact areas, drop volume, and Laplace excess pressure in drop-on-fibre system', *J. Colloid Interface Sci.* 1976 **57**(2) 488-492.

41 Mysels K J, 'Gravitational stability of sols. From Perrin to Usher', *Langmuir* 1992 **8**(12) 3191-3194.

42 Landau L D, Lifshitz E M, *Fluid Mechanics*, Oxford, Pergamon Press, 1984.

43 Reiss-Husson F, Luzzati V, 'The Structure of the Micellar Solutions of Some Amphiphilic Compounds in Pure Water as Determined by Absolute Small-Angle X-Ray Scattering Techniques', *J. Phys. Chem*. 1964 **68**(12) 3504-3511.

44 Eriksson J C, Ljunggren S, Claesson P M, 'Phenomenological theory of long-range hydrophobic attraction forces based on a square-gradient variational approach', *J. Chem. Soc. Faraday Trans. 2*, 1989 **85**(3) 163-176.

45 Angarska J K, Dimitrova B S, Danov K D, Kralchevsky P A, Ananthapadmanabhan K P, Lips A, 'Detection of the hydrophobic surface force in foam films by measurements of the critical thickness of film rupture', *Langmuir* 2004 **20**(5) 1799-1806.

46 Benson S W, *The Foundations of Chemical Kinetics*, New York, McGraw-Hill, 1960.

47 Lianos P, Lang J, Strazielle C, Zana R, 'Fluorescence probe study of oil-in-water microemulsions. 1. Effect of pentanol and dodecane or toluene on some properties of sodium dodecyl sulfate micelles', *J. Phys. Chem.* 1982 **86**(6) 1019-1025.

48 Almgren M, Swarup S, 'Size of sodium dodecyl sulfate micelles in the presence of additives. 2. Aromatic and saturated hydrocarbons', *J. Phys. Chem.* 1982 **86**(21) 4212-4216.

49 Bayer O, Hoffman H, Ulbricht W, Thurn H, 'The influence of solubilized additives on surfactant solutions with rodlike micelles', *Adv. Colloid Interface Sci.* 1986 **26**(1) 177-203.

50 Reekmans S, Luo H, van der Auweraer M, de Schryver F C, 'Influence of alcohols and alkanes on the aggregation behavior of ionic surfactants in water', *Langmuir* 1990 **6**(3) 628-637.

51 Zhao G-X, Li X-G, 'Solubilization of n-octane and n-octanol by a mixed aqueous solution of cationic-anionic surfactants', *J. Colloid Interface Sci.* 1991 **144**(1) 185-190.

52 Abe M, Tokuoka Y, Uchiyama H, Ogino K, Scamehorn J F, Christian S D, 'Expansion of mixed anionic–non-ionic micelles caused by solubilization of organic solutes', *Colloids Surf.* 1992 **67**(1) 37-43.

53 Lindemuth P M, Bertrand G L, 'Calorimetric observations of the transition of spherical to rodlike micelles with solubilized organic additives', *J. Phys. Chem.* 1993 **97**(29) 7769-7773.

54 Kumar S, Aswal V K, Singh H N, Goyal P S, Kabir-ud-Din, 'Growth of sodium dodecyl sulfate micelles in the presence of n-octylamine', *Langmuir* 1994 **10**(11) 4069-4072.

55 Alargova R G, Petkov J T, Petsev D N, Ivanov I B, Broze G, Mehreteab A, 'Light scattering study of sodium dodecyl polyoxyethylene-2-sulfate micelles in the presence of multivalent counterions', *Langmuir* 1995 **11**(5) 1530-1536.

56 Dunaway C S, Christian S D, Scamehorn J F, 'Overview and history of the study of solubilization', in Christian S D, and Scamehorn J F, *Solubilization in Surfactant Aggregates*, New York, Dekker M, 1995 Chapter 1.

57 Törnblom M, Henriksson U, 'Effect of solubilization of aliphatic hydrocarbons on size and shape of rodlike C_{16}TABr micelles studied by ^{2}H NMR relaxation', *J. Phys. Chem. B* 1997 **101**(31) 6028-6035.

58 Hedin N, Sitnikov R, Furo I, Henriksson U, Regev O, 'Shape changes of C_{16}TABr micelles on benzene solubilization', *J. Phys. Chem. B* 1999 **103**(44) 9631-9639.

59 Kim J-H, Domach M M, Tilton R D, 'Pyrene solubilization capacity in octaethylene glycol monododecyl ether ($C_{12}E_8$) micelles', *Colloids Surf. A* 1999 **150**(1-3) 55-68.

60 Cerichelli G, Mancini G, 'Role of counterions in the solubilization of benzene by cetyltrimethylammonium aggregates. A multinuclear NMR investigation', *Langmuir* 2000 **16**(1) 182-187.

61 Nagarajan R, 'Solubilization in aqueous solutions of amphiphiles', *Curr. Opin. Colloid Interface Sci.* 1996 **1**(4) 391-401.

62 Nagarajan R, 'Solubilization by amphiphilar aggregates', *Curr. Opin. Colloid Interface Sci.* 1997 **2**(3) 282-293.

63 Berne B J, Pecora R, *Dynamic Light Scattering with Applications to Chemistry, Biology and Physics*, New York, Wiley, 1976.

64 Bernheim-Groswasser A, Wachtel E, Talmon Y, 'Micellar growth, network formation, and criticality in aqueous solutions of the nonionic surfactant $C_{12}E_5$', *Langmuir* 2000 **16**(9) 4131-4140.

65 Bieze T W N, Barnes A C, Huige C J M, Enderby J E, Leyte J C, 'Distribution of water around poly(ethylene oxide): A neutron diffraction study', *J. Phys. Chem.* 1994 **98**(26) 6568-6576.

66 Garti N, Aserin A, Ezrahi S, Tiunova I, Berkovic G, 'Water behavior in nonionic surfactant systems I: Subzero temperature behavior of water in nonionic microemulsions studied by DSC', *J. Colloid Interface Sci.* 1996 **178**(1) 60-68.

67 Brenner H, 'Rheology of a dilute suspension of axisymmetric Brownian particles', *Int. J. Multiphase Flow* 1974 **1**(2) 195-341.

68 Kabalnov A S, 'Can micelles mediate a mass transfer between oil droplets?', *Langmuir* 1994 10(3) 680-684.

69 Taylor P. 'Ostwald ripening in emulsions', *Colloids Surf. A* 1995 **99**(2-3), 175-185.

70 Soma J, Papadopulos K D, 'Ostwald ripening in sodium dodecyl sulfate-stabilized decane-in-water emulsions', *J. Colloid Interface Sci.* 1996 **181**(1) 225-231.

71 Alargova R G, Ivanova V P, Kralchevsky P A, Mehreteab A, Broze G, 'Growth of rod-like micelles in anionic surfactant solutions in the presence of Ca^{2+} counterions', *Colloids Surf. A* 1998 **142**(2-3) 201-218.

72 Alargova R G, Danov K D, Kralchevsky P A, Broze G, Mehreteab A, 'Growth of giant rodlike micelles of ionic surfactant in the presence of Al^{3+} counterions', *Langmuir* 1998 **14**(15) 4036-4049.

73 Danov K D, Kralchevska, S D, Denkov N D, Kralchevsky P A, 'Kinetics of triglyceride solubilization in ionic surfactant solutions, promoted by block copolymers and trivalent counterions', *J. Colloid Interface Sci*. 2004 – to be submitted.